

This is a preprint of an article accepted for publication in the ASCE Journal of Engineering Mechanics on June 4 2009. The published article is available online at [ascelibrary.org/doi/abs/10.1061/\(ASCE\)EM.1943-7889.0000064](http://ascelibrary.org/doi/abs/10.1061/(ASCE)EM.1943-7889.0000064)

To be cited as: Bouaanani N., Perrault C. 2010. Practical formulas for frequency domain analysis of earthquake-induced dam-reservoir interaction. ASCE Journal of Engineering Mechanics, Vol. 136, No. 1, 107-119.

Practical Formulas for Frequency Domain Analysis of Earthquake Induced Dam-Reservoir Interaction

Najib Bouaanani¹ and Charles Perrault²

ABSTRACT

Dam-reservoir dynamic interactions are complex phenomena requiring advanced mathematical and numerical modeling. Although available sophisticated techniques can handle many aspects of these phenomena, simplified procedures are useful and still needed to globally evaluate the dynamic response of dam-reservoir systems. This paper presents and validates an original practical procedure to investigate earthquake induced dam-reservoir interaction in the frequency domain, including the effects of dam flexibility, water compressibility and reservoir bottom wave absorption. The procedure relates hydrodynamic pressure due to any deflected modal response of a 2D gravity dam on a rigid foundation to hydrodynamic pressure caused by a horizontal rigid body motion. New analytical expressions that can be easily programmed in a spreadsheet package or implemented in a dam structural analysis program are also proposed to conduct simplified fundamental mode earthquake analysis of gravity dams. The techniques presented can be efficiently used to provide valuable insight into the effects and relative importance of the various parameters involved in the dynamic response of dam-reservoir systems. Although the mathematical derivations and closed-form expressions developed were applied to dam-reservoir systems herein, they can be easily adapted to other fluid-structure interaction problems.

CE Database Subject headings: Hydrodynamic pressure; Dam safety; Seismic effects; Earthquake engineering; Reservoirs; Closed form solutions; Frequency response.

¹ Professor, Department of Civil, Geological and Mining Engineering, École Polytechnique de Montréal, Montréal, QC H3C 3A7, Canada
Corresponding author. E-mail: najib.bouaanani@polymtl.ca

² Research assistant, Department of Civil, Geological and Mining Engineering, École Polytechnique de Montréal, Montréal, QC H3C 3A7, Canada.

1 Introduction

Reliable and accurate prediction of hydrodynamic pressure is of utmost importance to the safety evaluation of hydraulic structures in earthquake prone areas. Significant research has been devoted to understand this type of loading since the pioneering work of Westergaard (Westergaard 1933). In Westergaard's solution, hydrodynamic pressure on a dam face is modeled as a heightwise added mass distribution obtained by neglecting dam flexibility and water compressibility. This added mass concept has been widely used for several decades to design earthquake resistant gravity dams. Chopra and collaborators contributed significantly to the understanding of fluid-structure interaction in dam engineering (Chopra 1968; Chopra 1970; Chakrabarti and Chopra 1973; Chopra 1978). They developed procedures to account for the effects of dam deformability and water compressibility in earthquake excited dam-reservoir systems. These techniques were refined later to account for reservoir bottom wave absorption and dam-foundation interaction (Fenves and Chopra 1985; Fenves and Chopra 1987).

The developments proposed by Chopra and collaborators have been extensively used worldwide for design and safety evaluation of concrete dams. These methods could be cast into two categories: (i) simplified procedures in which the fundamental vibration mode response of a dam-reservoir-foundation system is used to investigate most significant factors influencing the seismic behavior, and (ii) more sophisticated time history analysis procedures based on a coupled field solution through sub-structuring of the dam-reservoir-foundation system. The latter techniques were implemented in finite element codes specialized in two- and three-dimensional analyses of concrete gravity dams (Fenves and Chopra 1984; Fok et al. 1986). Some of these codes were used recently to validate forced-vibration testing of concrete gravity and arch dams (Proulx et al. 2001; Bouaanani et al. 2002). During the last three decades, several researchers developed advanced analytical and numerical frequency-domain and time-domain approaches to model dynamic dam-reservoir-foundation interactions (Saini et al. 1978; Liu and Cheng 1984; Tsai and Lee 1987; Humar 1988; Maeso et al. 2004). Most of these methods make use of finite elements, boundary elements or a mix of both.

Dynamic dam-reservoir interactions are complex phenomena requiring advanced mathematical and numerical modeling. Although the available sophisticated techniques can handle many aspects of these phenomena, simplified procedures are useful and still needed to globally evaluate the dynamic response of dam-reservoir systems, namely for preliminary design or safety evaluation of concrete dams. In a previous work, the first author proposed a simplified closed-form formulation for earthquake-induced hydrodynamic pressure on concrete dams (Bouaanani et al. 2003). The method includes the effects of water compressibility and reservoir bottom wave absorption. The influence of dam deformability was however neglected and therefore the total hydrodynamic pressure exerted on a dam during an earthquake and the associated response quantities could not be evaluated. The main purpose of this work is to develop a new closed-form formulation where the rigid dam restricting assumption is waived.

2 Theoretical Formulation

A triangular 2D gravity dam cross-section was used by Chopra et al. (Chopra 1970; Fenves and Chopra 1985) to illustrate the application of the simplified and numerical techniques they proposed. This idealized dam section is considered herein for convenient reference. The geometry of the dam-reservoir system is shown in Fig. 1. The dam has a total height H_s and it impounds a semi-infinite reservoir of constant depth H_r . Wave absorption due to sediments that may be deposited at reservoir bottom is also considered. A Cartesian coordinate system with axes x and y with origin at the heel of the structure is adopted and the following main assumptions are made : (i) the dam and the water are assumed to have a linear elastic behavior; (ii) the dam foundation is assumed rigid; (iii) the water in the reservoir is compressible and inviscid, with its motion irrotational and limited to small amplitudes; and (iv) gravity surface waves are neglected. The hydrodynamic pressure $p(x, y, t)$ in the reservoir (in excess of the hydrostatic pressure) obeys the following wave equations

$$\frac{\partial p}{\partial x} = -\rho_r \frac{\partial^2 u_r}{\partial t^2} \quad (1)$$

$$\frac{\partial p}{\partial y} = -\rho_r \frac{\partial^2 v_r}{\partial t^2} \quad (2)$$

$$\frac{\partial^2 p}{\partial x^2} + \frac{\partial^2 p}{\partial y^2} = \frac{1}{C_r^2} \frac{\partial^2 p}{\partial t^2} \quad (3)$$

where u_r and v_r are the x and y components of the displacement of a water particle, respectively; t is the time variable; ρ_r the mass density of water and C_r the velocity of sound in water. Considering harmonic ground motions : horizontal $\ddot{x}_g(t) = a_g^{(x)} e^{i\omega t}$, and vertical $\ddot{y}_g(t) = a_g^{(y)} e^{i\omega t}$, the hydrodynamic pressure in the reservoir can be expressed in the frequency domain as $p^{(\zeta)}(x, y, t) = \bar{p}^{(\zeta)}(x, y, \omega) e^{i\omega t}$, where the superscript (ζ) denotes the corresponding direction x or y , ω the exciting frequency, and $\bar{p}^{(\zeta)}(x, y, \omega)$ the complex-valued frequency response function. Introducing this transformation into Eq. (3) yields the classical Helmholtz equations

$$\frac{\partial^2 \bar{p}^{(\zeta)}}{\partial x^2} + \frac{\partial^2 \bar{p}^{(\zeta)}}{\partial y^2} + \frac{\omega^2}{C_r^2} \bar{p}^{(\zeta)} = 0 \quad \zeta = x, y \quad (4)$$

The frequency response function of structural displacement and acceleration components along earthquake excitation directions $\zeta = x, y$ can be expressed as

$$\bar{u}^{(\zeta)}(x, y, \omega) = \sum_{j=1}^{N_s} \psi_j^{(x)}(x, y) \bar{Z}_j^{(\zeta)}(\omega); \quad \bar{\ddot{u}}^{(\zeta)}(x, y, \omega) = -\omega^2 \sum_{j=1}^{N_s} \psi_j^{(x)}(x, y) \bar{Z}_j^{(\zeta)}(\omega) \quad (5)$$

$$\bar{v}^{(\zeta)}(x, y, \omega) = \sum_{j=1}^{N_s} \psi_j^{(y)}(x, y) \bar{Z}_j^{(\zeta)}(\omega); \quad \bar{\ddot{v}}^{(\zeta)}(x, y, \omega) = -\omega^2 \sum_{j=1}^{N_s} \psi_j^{(y)}(x, y) \bar{Z}_j^{(\zeta)}(\omega) \quad (6)$$

where $\bar{u}^{(\zeta)}$ and $\bar{v}^{(\zeta)}$ denote the horizontal and vertical displacements, respectively, $\ddot{\bar{u}}^{(\zeta)}$ and $\ddot{\bar{v}}^{(\zeta)}$ the horizontal and vertical accelerations, respectively, $\psi_j^{(x)}$ and $\psi_j^{(y)}$ the x - and y -components of the j^{th} structural mode shape, $\bar{Z}_j^{(\zeta)}$ the generalized coordinate along earthquake excitation direction ζ , and N_s the total number of mode shapes included in the analysis.

The complex-valued hydrodynamic pressure frequency response functions $\bar{p}^{(\zeta)}$ along directions $\zeta = x, y$ can be expressed as (Fenves and Chopra 1984)

$$\bar{p}^{(\zeta)}(x, y, \omega) = \bar{p}_0^{(\zeta)}(x, y, \omega) - \omega^2 \sum_{j=1}^{N_s} \bar{Z}_j^{(\zeta)}(\omega) \bar{p}_j(x, y, \omega); \quad \zeta = x, y \quad (7)$$

where $\bar{p}_0^{(\zeta)}$ is the frequency response function for hydrodynamic pressure at rigid dam face due to ground acceleration along $\zeta = x, y$ direction, and where \bar{p}_j is the frequency response for hydrodynamic pressure due to horizontal acceleration $\psi_j^{(x)}(y) = \psi_j^{(x)}(0, y)$ of the dam upstream face. Throughout this paper, hydrodynamic pressures $\bar{p}_0^{(\zeta)}$ and \bar{p}_j will be referred to as the “rigid” and the “flexible” parts of the total hydrodynamic pressure \bar{p} , respectively.

The boundary conditions to be satisfied by frequency response functions $\bar{p}_0^{(x)}$, $\bar{p}_0^{(y)}$ and \bar{p}_j are

– At the dam-reservoir interface

$$\frac{\partial \bar{p}_0^{(x)}}{\partial x}(0, y, \omega) = -\rho_r a_g^{(x)} \quad (8)$$

$$\frac{\partial \bar{p}_0^{(y)}}{\partial x}(0, y, \omega) = 0 \quad (9)$$

$$\frac{\partial \bar{p}_j}{\partial x}(0, y, \omega) = -\rho_r \psi_j^{(x)}(y) \quad (10)$$

– At the reservoir bottom

$$\frac{\partial \bar{p}_0^{(x)}}{\partial y}(x, 0, \omega) = i\omega q \bar{p}_0^{(x)}(x, 0, \omega) \quad (11)$$

$$\frac{\partial \bar{p}_0^{(y)}}{\partial y}(x, 0, \omega) = -\rho_r a_g^{(y)} + i\omega q \bar{p}_0^{(y)}(x, 0, \omega) \quad (12)$$

$$\frac{\partial \bar{p}_j}{\partial y}(x, 0, \omega) = i\omega q \bar{p}_j(x, 0, \omega) \quad (13)$$

where q is a damping coefficient defined at the reservoir bottom as

$$q = \frac{\rho_r}{\rho_f C_f} \quad (14)$$

and where ρ_f and C_f denote the mass density and the compression-wave velocity within the dam-reservoir foundation, respectively. The portion of the wave amplitude reflected back to the reservoir

can then be represented by the wave reflection coefficient α defined by

$$\alpha = \frac{1 - q C_r}{1 + q C_r} \quad (15)$$

where α may vary from 0, for full wave absorption, to 1, for full wave reflection.

– At the reservoir free surface

$$\bar{p}_0^{(x)}(x, H_r, \omega) = \bar{p}_0^{(y)}(x, H_r, \omega) = \bar{p}_j(x, H_r, \omega) = 0 \quad (16)$$

The complex frequency response functions of the rigid and flexible parts of hydrodynamic pressure, $\bar{p}_0^{(x)}$ and \bar{p}_j , can be expressed as the summation of N_r response functions $\bar{p}_{0n}^{(x)}$ and \bar{p}_{jn} corresponding each to a reservoir mode n

$$\bar{p}_0^{(x)}(x, y, \omega) = \sum_{n=1}^{N_r} \bar{p}_{0n}^{(x)}(x, y, \omega) \quad (17)$$

$$\bar{p}_j(x, y, \omega) = \sum_{n=1}^{N_r} \bar{p}_{jn}(x, y, \omega) \quad (18)$$

Frequency response functions $\bar{p}_{0n}^{(x)}$ and \bar{p}_{jn} are given by

$$\bar{p}_{0n}^{(x)}(x, y, \omega) = -2\rho_r a_g^{(x)} H_r \frac{\lambda_n^2(\omega)}{\beta_n(\omega)} \frac{I_{0n}(\omega)}{\kappa_n(\omega)} e^{\kappa_n(\omega)x} Y_n(y, \omega) \quad (19)$$

$$\bar{p}_{jn}(x, y, \omega) = -2\rho_r H_r \frac{\lambda_n^2(\omega)}{\beta_n(\omega)} \frac{I_{jn}(\omega)}{\kappa_n(\omega)} e^{\kappa_n(\omega)x} Y_n(y, \omega) \quad (20)$$

where λ_n and Y_n are complex-valued frequency dependent eigenvalues and orthogonal eigenfunctions satisfying, for each reservoir mode n

$$e^{2i\lambda_n(\omega)H_r} = -\frac{\lambda_n(\omega) - \omega q}{\lambda_n(\omega) + \omega q} \quad (21)$$

$$Y_n(y, \omega) = \frac{[\lambda_n(\omega) - \omega q] e^{-i\lambda_n(\omega)y} + [\lambda_n(\omega) + \omega q] e^{i\lambda_n(\omega)y}}{2\lambda_n(\omega)} \quad (22)$$

and where the terms β_n , κ_n , I_{0n} and I_{jn} are given by

$$\beta_n(\omega) = H_r [\lambda_n^2(\omega) - \omega^2 q^2] + i\omega q \quad (23)$$

$$\kappa_n(\omega) = \sqrt{\lambda_n^2(\omega) - \frac{\omega^2}{C_r^2}} \quad (24)$$

$$I_{0n}(\omega) = \frac{1}{H_r} \int_0^{H_r} Y_n(y, \omega) \, dy \quad (25)$$

$$I_{jn}(\omega) = \frac{1}{H_r} \int_0^{H_r} \psi_j^{(x)}(y) Y_n(y, \omega) \, dy \quad (26)$$

Using Eqs. (21) and (22), the integral I_{0n} given by Eq. (25) can be determined as

$$I_{0n}(\omega) = \frac{i e^{-i \lambda_n H_r}}{\lambda_n^2 H_r} \left(\lambda_n - \omega q + \omega q e^{i \lambda_n H_r} \right) \quad (27)$$

where $\lambda_n(\omega)$ is noted λ_n for brevity.

The complex frequency response function of hydrodynamic pressure $\bar{p}_0^{(y)}$ is independent of x -coordinate and can be expressed as (Fenves and Chopra 1984)

$$\bar{p}_0^{(y)}(y, \omega) = \frac{\rho_r C_r a_g^{(y)}}{\omega \left(\cos \frac{\omega H_r}{C_r} + i q C_r \sin \frac{\omega H_r}{C_r} \right)} \sin \frac{\omega (H_r - y)}{C_r} \quad (28)$$

A relationship between the rigid and flexible parts of hydrodynamic pressure is investigated next. We assume that the x -component of structural mode shape ψ_j can be approximated as a polynomial function

$$\psi_j^{(x)}(y) = \sum_k a_k \left(\frac{y}{H_s} \right)^k \quad (29)$$

where y is the coordinate varying along the height of the structure measured from its base. The coefficients a_k can be determined based on a finite element analysis of the structure as illustrated in Fig. 2. Simplified formulas approximating the fundamental mode shape of gravity dams as the one proposed by Chopra (1970) can also be used. On substituting Eq. (29) into the integral I_{jn} given by Eq. (26), we have

$$\begin{aligned} I_{jn}(\omega) &= \frac{1}{H_r} \int_0^{H_r} \psi_j^{(x)}(y) Y_n(y, \omega) \, dy \\ &= \frac{1}{H_r} \sum_k \frac{a_k}{H_s^k} \int_0^{H_r} y^k Y_n(y, \omega) \, dy \end{aligned} \quad (30)$$

To alleviate the notation, we introduce the complex-valued function Λ_m defined by

$$\Lambda_m(z) = \frac{z^m}{m!} \quad (31)$$

where z and m are complex and integer numbers, respectively. Using integration by parts, we show

that

$$\int_0^{H_r} y^{2k} Y_n(y, \omega) dy = \frac{i\omega q}{\lambda_n^2} \frac{(-1)^k}{\Lambda_{2k}(\lambda_n)} + \left[H_r I_{0n} - \frac{i\omega q}{\lambda_n^2} \right] \sum_{\ell=0}^k (-1)^{k-\ell} \frac{\Lambda_{2\ell}(\lambda_n H_r)}{\Lambda_{2k}(\lambda_n)} \quad (32)$$

$$\int_0^{H_r} y^{2k+1} Y_n(y, \omega) dy = -\frac{(-1)^k}{\lambda_n \Lambda_{2k+1}(\lambda_n)} + \left[H_r I_{0n} - \frac{i\omega q}{\lambda_n^2} \right] \sum_{\ell=0}^k (-1)^{k-\ell} \frac{\Lambda_{2\ell+1}(\lambda_n H_r)}{\Lambda_{2k+1}(\lambda_n)} \quad (33)$$

Eq. (30) becomes then

$$I_{jn}(\omega) = F_{jn}(\omega) I_{0n}(\omega) + G_{jn}(\omega) \quad (34)$$

where

$$F_{jn}(\omega) = \sum_k \left\{ \left[\sum_{\ell=0}^k (-1)^{k-\ell} \frac{\Lambda_{2\ell}(\lambda_n H_r)}{\Lambda_{2k}(\lambda_n H_s)} \right] a_{2k} + \left[\sum_{\ell=0}^k (-1)^{k-\ell} \frac{\Lambda_{2\ell+1}(\lambda_n H_r)}{\Lambda_{2k+1}(\lambda_n H_s)} \right] a_{2k+1} \right\} \quad (35)$$

$$G_{jn}(\omega) = -\frac{i\omega q}{\lambda_n^2 H_r} F_{jn}(\omega) + \frac{1}{\lambda_n H_r} \sum_k \left\{ \left[\frac{i\omega q}{\lambda_n} \frac{(-1)^k}{\Lambda_{2k}(\lambda_n H_s)} \right] a_{2k} - \left[\frac{(-1)^k}{\Lambda_{2k+1}(\lambda_n H_s)} \right] a_{2k+1} \right\} \quad (36)$$

For example, if a cubic profile is used to approximate $\psi_j^{(x)}$

$$\psi_j^{(x)}(y) = a_1 \frac{y}{H_s} + a_2 \left(\frac{y}{H_s} \right)^2 + a_3 \left(\frac{y}{H_s} \right)^3 \quad (37)$$

Eqs. (35) and (36) simplify to

$$F_{jn}(\omega) = \psi_j^{(x)}(H_r) - \frac{2}{\lambda_n^2 H_s^2} a_2 - \frac{6H_r}{\lambda_n^2 H_s^3} a_3 \quad (38)$$

$$G_{jn}(\omega) = -\frac{i\omega q}{\lambda_n^2 H_r} \left[\psi_j^{(x)}(H_r) - \frac{6H_r}{\lambda_n^2 H_s^3} a_3 \right] - \frac{1}{\lambda_n^2 H_r H_s} a_1 + \frac{6}{\lambda_n^4 H_r H_s^3} a_3$$

To closely interpolate various modal shapes, F_{jn} and G_{jn} expressions developed using quadratic to quintic approximations are given in Appendix A.

Getting back to the frequency response function \bar{p}_{jn} of the the flexible part of hydrodynamic pressure and substituting Eq. (34) into Eq. (20), we show that

$$\bar{p}_{jn}(x, y, \omega) = \frac{\bar{p}_{0n}^{(x)}(x, y, \omega)}{a_g^{(x)}} \left[F_{jn}(\omega) + \frac{G_{jn}(\omega)}{I_{0n}(\omega)} \right] \quad (39)$$

This original and important relation relates the flexible and rigid parts of hydrodynamic pressure at a given reservoir mode n to the vibration of the structure along a given mode shape ψ_j . Therefore, if frequency response function $\bar{p}_{0n}^{(x)}$ is known for a given reservoir mode n , the effect of a given structural

mode shape $\psi_j^{(x)}$ can be obtained using Eq. (39) to find frequency response function \bar{p}_{jn} corresponding to the same reservoir mode n . Summation over the number of reservoir modes N_r yields the total rigid and flexible parts of hydrodynamic pressure according to Eqs. (17) and (18), respectively.

For purpose of illustration, this formulation is applied to the dam-reservoir system shown in Fig. 1. We consider a unit horizontal harmonic ground motion $\ddot{x}_g(t) = e^{i\omega t}$, a one-meter wide dam section of height $H_s = 121.92$ m (400 ft), a downstream slope of 0.8 and a vertical upstream face. The following dam material properties are selected: a modulus of elasticity $E_s = 25$ GPa; a Poisson's ratio $\nu_s = 0.2$; and a mass density $\rho_s = 2400$ kg/m³. Water is assumed compressible, with a velocity of pressure waves $C_r = 1440$ m/s, and a mass density $\rho_r = 1000$ kg/m³. We denote by $g = 9.81$ m/s² the gravitational acceleration. The absolute value of frequency response functions of the flexible part of hydrodynamic pressure at dam heel due to structural mode shapes ψ_1 to ψ_4 are determined. Two levels of reservoir bottom wave absorption $\alpha = 0.95$ and $\alpha = 0.65$ are considered. Mode shapes are obtained from a plane stress finite element analysis of the dam cross-section carried out using the software ADINA (2008). These refined mode shapes are included in the classical formulation described previously. The proposed method is applied using cubic to quintic expressions (Appendix A) to appropriately approximate the modal shapes at dam face. Fig. 3 compares the results obtained using the proposed approximate method to those of the classical formulation for a full reservoir case, i.e. $H_r = H_s$, and frequency ratios ω/ω_0 varying from 0 to 4, where $\omega_0 = \pi C_r/(2H_r)$ denotes the natural frequency of the full reservoir. As can be seen, both methods yield practically identical frequency response curves. We also observe that once a minimum approximation order is fixed to match a given mode shape, increasing the order of the approximation has virtually no effect on the results.

3 Practical Closed-form Expressions

The eigenvalue problem given by Eq. (21) has to be solved for eigenvalues λ_n at each excitation frequency ω in the range of interest. For this purpose, numerical iterative techniques such as Newton-Raphson method have to be programmed as done in the EAGD computer code (Fenves and Chopra 1984). Such methods also require an initial guess of the eigenvalues and would converge only after a certain number of iterations. In this paper, closed-form expressions that can be used to directly obtain the eigenvalues λ_n are developed. The proposed formulas can be efficiently implemented in a practical dam structural analysis without recourse to iterative solutions or complex programming. This approach also allows more insight into the relative contributions of different parameters to the overall response of a dam-reservoir system. Once the eigenvalues are determined, practical analytical expressions to evaluate complex-valued frequency response functions of the rigid and hydrodynamic parts of hydrodynamic pressure can be developed.

Performing derivation with respect to ω , we show that Eq. (21) is equivalent to the non-linear differ-

ential equation

$$\frac{d\lambda_n}{d\omega} = \frac{\lambda_n}{\omega + i H_r q \left(\omega^2 - \frac{\lambda_n^2}{q^2} \right)} \quad (40)$$

We also demonstrate through numerical simulations that for large and moderate values of the reflection coefficient, i.e. $\alpha \geq 0.5$, the term ω^2 is relatively small compared to the other terms in Eq. (40), and that it can be dropped without introducing significant error as will be shown later. Hence, we can assume that under some conditions that define the range of validity of this approximation, Eq. (40) simplifies to

$$\frac{d\lambda_n}{d\omega} = \frac{\lambda_n q}{\omega q - i H_r \lambda_n^2} \quad (41)$$

Using the root $\lambda_n(0) = \frac{(2n-1)\pi}{2H_r}$ of Eq. (21) at frequency $\omega=0$, and integrating Eq. (41) between 0 and ω yields the approximate solution for eigenvalues λ_n

$$\lambda_n(\omega) = \frac{(2n-1)\pi}{4H_r} + \sqrt{\frac{(2n-1)^2 \pi^2}{(4H_r)^2} + i \frac{\omega q}{H_r}} \quad (42)$$

Eq. (42) can then be introduced into Eqs. (22) to (24) and Eq. (27) to obtain the parameters Y_n , β_n , κ_n and I_{0n} required to determine frequency response functions \bar{p}_{0n} and $\bar{p}_0^{(x)}$ according to Eqs. (19) and (17), respectively.

For practical programming, we propose the following simplified expressions to evaluate frequency response function $\bar{p}_{0n}^{(x)}$ of the rigid part of hydrodynamic pressure at dam face

$$\begin{aligned} \bar{p}_{0n}^{(x)}(0, y, \omega) &= -2\rho_r a_g^{(x)} H_r \frac{(S_3 + i S_4)^2 (S_{15} + i S_{16}) (S_{11} + i S_{12})}{\left[H_r (S_3 \sqrt{S_0} - \omega^2 q^2) + i (2H_r S_3 S_4 + \omega q) \right] (S_7 + i S_8)} \\ &= -\frac{2\rho_r a_g^{(x)} H_r}{S_7^2 + S_8^2} \left[(S_{11} S_{20} - S_{12} S_{19}) + i (S_{11} S_{19} + S_{12} S_{20}) \right] \end{aligned} \quad (43)$$

where the coefficients S_j , $j = 1 \dots 20$, are derived analytically as

$$S_1 = \frac{(2n-1)^2 \pi^2}{4H_r^2}; \quad S_2 = 4\sqrt{S_1^2 + 16 \frac{\omega^2 q^2}{H_r^2}} \quad (44)$$

$$S_3 = \frac{1}{2} \left[\sqrt{S_1} + \frac{1}{4} \sqrt{2(S_2 + 4S_1)} \right]; \quad S_4 = \frac{1}{8} \sqrt{2(S_2 - 4S_1)} \quad (45)$$

$$S_5 = 4 \left(S_3 \sqrt{S_1} - \frac{\omega^2}{C^2} \right); \quad S_6 = \sqrt{S_5^2 + 64 S_3^2 S_4^2} \quad (46)$$

$$S_7 = \frac{1}{4}\sqrt{2(S_5 + S_6)}; \quad S_8 = \frac{1}{4}\sqrt{2(S_6 - S_5)} \quad (47)$$

$$S_9 = \left[(S_3 + \omega q) e^{-S_4 y} + (S_3 - \omega q) e^{S_4 y} \right] \cos(S_3 y) + \left[e^{S_4 y} - e^{-S_4 y} \right] S_4 \sin(S_3 y) \quad (48)$$

$$S_{10} = \left[(S_3 + \omega q) e^{-S_4 y} - (S_3 - \omega q) e^{S_4 y} \right] \sin(S_3 y) + \left[e^{-S_4 y} + e^{S_4 y} \right] S_4 \cos(S_3 y) \quad (49)$$

$$S_{11} = \frac{S_9 S_3 + S_{10} S_4}{2(S_3^2 + S_4^2)}; \quad S_{12} = \frac{S_{10} S_3 - S_9 S_4}{2(S_3^2 + S_4^2)} \quad (50)$$

$$S_{13} = \frac{S_3 \left[\sqrt{S_1} \sin(H_r S_3) + 2S_4 \cos(H_r S_3) \right]}{(S_3^2 + S_4^2)^2} e^{H_r S_4} \quad (51)$$

$$S_{14} = \frac{S_3 \left[\sqrt{S_1} \cos(H_r S_3) - 2S_4 \sin(H_r S_3) \right]}{(S_3^2 + S_4^2)^2} e^{H_r S_4} \quad (52)$$

$$S_{15} = \frac{S_{13}}{H_r} \left[S_3 - \omega q + \omega q e^{-H_r S_4} \cos(H_r S_3) \right] - \frac{S_{14}}{H_r} \left[S_4 + \omega q e^{-H_r S_4} \sin(H_r S_3) \right] \quad (53)$$

$$S_{16} = \frac{S_{14}}{H_r} \left[S_3 - \omega q + \omega q e^{-H_r S_4} \cos(H_r S_3) \right] + \frac{S_{13}}{H_r} \left[S_4 + \omega q e^{-H_r S_4} \sin(H_r S_3) \right] \quad (54)$$

$$S_{17} = \frac{H_r S_3 (S_3 \sqrt{S_1} - \omega^2 q^2) (S_{15} \sqrt{S_1} - 2S_4 S_{16}) + S_3 (2H_r S_3 S_4 + \omega q) (2S_4 S_{15} + S_{16} \sqrt{S_1})}{\left[H_r (S_3 \sqrt{S_1} - \omega^2 q^2) \right]^2 + (2H_r S_3 S_4 + \omega q)^2} \quad (55)$$

$$S_{18} = \frac{H_r S_3 (S_3 \sqrt{S_1} - \omega^2 q^2) (2S_4 S_{15} + S_{16} \sqrt{S_1}) - S_3 (2H_r S_3 S_4 + \omega q) (S_{15} \sqrt{S_1} - 2S_4 S_{16})}{\left[H_r (S_3 \sqrt{S_1} - \omega^2 q^2) \right]^2 + (2H_r S_3 S_4 + \omega q)^2} \quad (56)$$

$$S_{19} = S_8 S_{18} - S_7 S_{17}; \quad S_{20} = S_8 S_{17} + S_7 S_{18} \quad (57)$$

For a fully reflective reservoir bottom ($\alpha = 1$), the frequency response $\bar{p}_{0n}^{(x)}$ of the rigid part of hydrodynamic pressure at dam face is given by

$$\bar{p}_{0n}^{(x)}(0, y, \omega) = -4\rho_r a_g^{(x)} \frac{(-1)^{n-1} \cos \left[\frac{(2n-1)\pi y}{2H_r} \right]}{(2n-1)\pi \sqrt{\frac{(2n-1)^2 \pi^2}{4H_r^2} - \frac{\omega^2}{C_r^2}}} \quad (58)$$

Having estimated frequency response function $\bar{p}_{0n}^{(x)}$ according to Eq. (43) or (58), frequency response function \bar{p}_{1n} of the flexible part of hydrodynamic pressure corresponding to dam fundamental mode response $\psi_1^{(x)}$ can be obtained using Eq. (39). A cubic profile as in Eq. (37) should be adopted to appropriately match the fundamental mode shape at dam face. As shown in Appendix A, eigenvalues λ_n appear in the denominators of expressions F_{1n} and G_{1n} , with higher exponents as the order of the approximation increases. Therefore, to minimize the error introduced by the approximations used to obtain eigenvalues λ_n , mode shape profiles of orders higher than cubic need not be considered to study dam fundamental mode response using this simplified method.

To assess the validity and accuracy of the analytical expressions presented in this section, they are applied to the dam-reservoir system described previously (Fig. 1). Figs. 4 to 6 illustrate the frequency dependence of the real and imaginary parts of eigenvalues λ_n and parameters β_n and κ_n obtained for a full reservoir case and for different values of wave reflection coefficient α . In these Figures, the proposed closed-form formulation is compared to a numerical method based on a Newton-Raphson resolution scheme of Eq. (21). This technique will be referred to as the “classical method” in the rest of the paper. Results in Figs. 4 to 6 are determined for frequency ratios ω/ω_0 varying from 0 to 4, where $\omega_0 = \pi C_r/(2H_r)$ denotes the natural frequency of the full reservoir. Figs. 4 to 6 clearly show that the proposed method gives excellent results for high reflection coefficients α . The quality of the approximation slightly decreases with larger reservoir bottom wave absorption. The agreement between the two methods remains however very satisfactory even for values of α as low as 0.65. Minor discrepancies are found at high frequencies larger than $2\omega_0$ and would be less critical to typically short-period dam-reservoir systems. Recommended values for α generally lie between 0.9 and 1.0 for new dams, and between 0.75 and 0.90 for older dams. Larger α values are usually adopted for preliminary design purposes since they generally yield conservative results. The curves also confirm that, within the frequency interval of interest, the real parts of eigenvalues λ_n are virtually insensitive to frequency and reservoir bottom wave reflection as suggested by Eq. (42). The imaginary parts of the eigenvalues λ_n exhibit a linear variation, taking larger values with increasing frequency ratio and bottom wave absorption. Even for a high absorptive reservoir bottom, the approximation of the coefficients β_n and κ_n is excellent over the whole frequency range of interest.

Fig. 7 illustrates the absolute value of normalized hydrodynamic pressure frequency response functions $\bar{p}_0^{(x)}/(\rho_r g H_r)$ and $\bar{p}_1/(\rho_r g H_r)$ obtained at the heel of the dam for different values of wave reflection coefficient α . First, frequency response function $\bar{p}_{0n}^{(x)}$ of the rigid part of hydrodynamic pressure is determined using Eq. (43) or (58). Frequency response function \bar{p}_{1n} of the flexible part of hydrodynamic pressure due to dam vibration along its fundamental mode shape is obtained next according to Eq. (39). A cubic profile is chosen to approximate the first structural mode shape $\psi_1^{(x)}$ resulting from a plane stress finite element analysis of the dam cross-section carried out using the software ADINA (2008). Eq. (37) is used accordingly and coefficients F_{1n} and G_{1n} are calculated next by applying Eq. (38). Eqs. (17) and (18) are then used to compute the hydrodynamic pressure frequency response functions $\bar{p}_0^{(x)}/(\rho_r g H_r)$ and $\bar{p}_1/(\rho_r g H_r)$ including a sufficient number of reservoir modes N_r .

As shown in Fig. 7, an excellent agreement is observed from the comparison with the results obtained using the classical method for frequency response functions $\bar{p}_0^{(x)}/(\rho_r g H_r)$ corresponding to the rigid part of hydrodynamic pressure. The quality of the approximation does not decay as wave reflection coefficient decreases. Results for frequency response functions $\bar{p}_1/(\rho_r g H_r)$ corresponding to the flexible part of hydrodynamic pressure are also excellent, mainly for highly reflective reservoir bottoms. Slight discrepancies are observed for reservoirs with high reservoir bottom wave absorption, the agreement between the two methods remains however excellent for $\omega \leq \omega_0$ and still quite reasonable for higher frequency ratios. In all cases, the resonant frequencies are accurately predicted by the proposed method. We note that these results do not include the coupling between the vibration of the dam upstream face and the pressure modes of the reservoir. This interaction will be investigated in the next section.

4 Application to the Simplified Earthquake Analysis of Gravity Dams

In this section, the closed-form expressions developed above are implemented into a fundamental mode dynamic analysis that takes account of some significant factors influencing the seismic response of dam-reservoir systems. Fenves and Chopra (1984, 1985, 1987) proved indeed that the earthquake response of a dam-reservoir system can be efficiently investigated in the frequency domain through construction of an Equivalent Single Degree of Freedom (ESDOF) system. The effects of dam-reservoir interaction and reservoir bottom wave absorption are included through added frequency-dependent force, mass and damping. Fenves and Chopra (1987) presented numerical examples illustrating the use of the ESDOF system representation and discussed its limitations.

Considering the fundamental mode response of the dam and a horizontal ground excitation, Eq. (5) simplifies to

$$\bar{u}^{(x)}(x, y, \omega) = \psi_1^{(x)}(x, y) \bar{Z}_1^{(x)}(\omega); \quad \bar{\ddot{u}}^{(x)}(x, y, \omega) = -\omega^2 \psi_1^{(x)}(x, y) \bar{Z}_1^{(x)}(\omega) \quad (59)$$

Under unit horizontal harmonic ground motion $\ddot{x}_g(t) = e^{i\omega t}$, the vibrations of a dam-reservoir ESDOF system are governed in the frequency domain by

$$\left(-\omega^2 M_1 + i\omega C_1 + K_1 \right) \bar{Z}_1^{(x)}(\omega) = -L_1 + \int_0^{H_r} \bar{p}^{(x)}(0, y, \omega) \psi_1^{(x)}(y) dy \quad (60)$$

where the generalized mass M_1 , generalized damping C_1 , generalized stiffness K_1 and participation

factor L_1 of the ESDOF corresponding to the dam with an empty reservoir are given by

$$M_1 = \iint \rho_s(x, y) [\psi_1^{(x)}(x, y)]^2 dx dy + \iint \rho_s(x, y) [\psi_1^{(y)}(x, y)]^2 dx dy \quad (61)$$

$$C_1 = 2M_1\xi_1\omega_1 \quad (62)$$

$$K_1 = \omega_1^2 M_1 \quad (63)$$

$$L_1 = \iint \rho_s(x, y) \psi_1^{(x)}(x, y) dx dy \quad (64)$$

in which ρ_s is the mass density of the dam concrete, ξ_1 is the fraction of critical damping at the fundamental vibration mode of the dam with an empty reservoir, and ω_1 its fundamental natural vibration frequency. The integration over the area of the dam can be approximated by integration over its height, thus simplifying Eqs. (61) and (64) to

$$M_1 \approx \int_0^{H_s} \mu_s(y) [\psi_1^{(x)}(y)]^2 dy \quad (65)$$

$$L_1 \approx \int_0^{H_s} \mu_s(y) \psi_1^{(x)}(y) dy \quad (66)$$

where μ_s is the mass of the dam per unit height. Substituting Eq. (7) into Eq. (60) results in

$$\left[-\omega^2 M_1 + i\omega C_1 + K_1 + \omega^2 \int_0^{H_r} \bar{p}_1(0, y, \omega) \psi_1^{(x)}(y) dy \right] \bar{Z}_1^{(x)}(\omega) = -L_1 + \int_0^{H_r} \bar{p}_0^{(x)}(0, y, \omega) \psi_1^{(x)}(y) dy \quad (67)$$

which yields the generalized coordinate

$$\bar{Z}_1^{(x)}(\omega) = \frac{-L_1 - B_0(\omega)}{-\omega^2 \left(M_1 + \text{Re}[B_1(\omega)] \right) + i\omega \left(C_1 - \omega \text{Im}[B_1(\omega)] \right) + K_1} \quad (68)$$

in which

$$B_0(\omega) = - \int_0^{H_r} \bar{p}_0^{(x)}(0, y, \omega) \psi_1^{(x)}(y) dy = \sum_{n=1}^{N_r} B_{0n}(\omega) \quad (69)$$

$$B_1(\omega) = - \int_0^{H_r} \bar{p}_1(0, y, \omega) \psi_1^{(x)}(y) dy = \sum_{n=1}^{N_r} B_{1n}(\omega) \quad (70)$$

where we introduced the notation

$$B_{0n}(\omega) = - \int_0^{H_r} \bar{p}_{0n}^{(x)}(0, y, \omega) \psi_1^{(x)}(y) dy \quad (71)$$

$$B_{1n}(\omega) = - \int_0^{H_r} \bar{p}_{1n}(0, y, \omega) \psi_1^{(x)}(y) dy \quad (72)$$

These frequency-dependent hydrodynamic parameters account for the effects of dam-reservoir interaction and reservoir bottom wave absorption. The term B_0 can be interpreted as an added force, the

real part of B_1 as an added mass and the imaginary part of B_1 as an added damping (Fenves and Chopra 1984). Using Eq. (19), we obtain

$$B_{0n}(\omega) = 2\rho_r H_r \frac{\lambda_n^2(\omega)}{\beta_n(\omega)} \frac{I_{0n}(\omega)}{\kappa_n(\omega)} \int_0^{H_r} \psi_1^{(x)}(y) Y_n(y, \omega) dy \quad (73)$$

Substituting with I_{1n} according to Eq. (30) and then Eq. (34) yields

$$B_{0n}(\omega) = 2\rho_r H_r^2 \frac{\lambda_n^2(\omega)}{\beta_n(\omega)} \frac{I_{0n}(\omega)}{\kappa_n(\omega)} \left[F_{1n}(\omega) I_{0n}(\omega) + G_{1n}(\omega) \right] \quad (74)$$

and using the transformation of Eq. (39)

$$\begin{aligned} B_{1n}(\omega) &= \left[F_{1n}(\omega) + \frac{G_{1n}(\omega)}{I_{0n}(\omega)} \right] B_{0n}(\omega) \\ &= 2\rho_r H_r^2 \frac{\lambda_n^2(\omega)}{\beta_n(\omega) \kappa_n(\omega)} \left[F_{1n}(\omega) I_{0n}(\omega) + G_{1n}(\omega) \right]^2 \end{aligned} \quad (75)$$

The resulting values can be introduced into Eq. (68) to determine the generalized coordinate $\bar{Z}_1^{(x)}$ and then the displacement and acceleration frequency response functions according to Eq. (59). We note that for a fully reflective reservoir bottom ($\alpha = 1$), the hydrodynamic terms B_0 and B_1 are real-valued, and Eqs. (74) and (75) take the form

$$B_{0n}(\omega) = 4\rho_r H_r \frac{(-1)^{n-1} \left[2 \times (-1)^{n-1} F_{1n}(\omega) + (2n-1) \pi G_{1n}(\omega) \right]}{(2n-1)^2 \pi^2 \sqrt{\frac{(2n-1)^2 \pi^2}{4H_r^2} - \frac{\omega^2}{C_r^2}}} \quad (76)$$

and

$$B_{1n}(\omega) = 2\rho_r H_r \frac{\left[2 \times (-1)^{n-1} F_{1n}(\omega) + (2n-1) \pi G_{1n}(\omega) \right]^2}{(2n-1)^2 \pi^2 \sqrt{\frac{(2n-1)^2 \pi^2}{4H_r^2} - \frac{\omega^2}{C_r^2}}} \quad (77)$$

The effectiveness of the closed-form expressions developed previously in reproducing the dynamic response of a dam-reservoir system is investigated next. Fig. 8 presents the absolute value of the frequency response function of horizontal acceleration at dam crest obtained using the classical and the proposed methods. The responses are plotted against the frequency ratio ω/ω_1 where ω_1 is the fundamental vibration frequency of the dam on rigid foundation with an empty reservoir. This frequency can be estimated as (Fenves and Chopra 1987)

$$\omega_1 = \frac{2\pi \sqrt{E_s}}{0.38H_s} \quad (78)$$

where E_s is expressed in MPa and H_s in meters. To assess the influence of dam stiffness, two modulus of elasticity $E_s = 25$ GPa and $E_s = 35$ GPa are considered. A damping ratio $\xi_1 = 0.05$ is adopted. Fig. 8

clearly shows the excellent agreement between the classical formulation and the proposed method even for highly absorptive reservoirs. The same observation applies to the absolute value of the total hydrodynamic pressure frequency response functions at dam heel as illustrated in Fig. 9. To further investigate the influence of frequency ratio ω/ω_1 on the accuracy of the proposed method, Fig. 10 shows the absolute value of the total hydrodynamic pressure distributions over reservoir height, obtained for different frequency ratios ω/ω_1 and different values of reflection coefficient α . Again, we confirm the excellent agreement between the classical formulation and the proposed method.

An important parameter in the analysis of dam-reservoir interaction problems is the first resonant vibration frequency of the combined fluid and structure subsystems. This parameter can be evaluated by plotting the fundamental mode response functions given by Eq. (59) and identifying the frequency $\tilde{\omega}_r$ corresponding to the first resonant peak. Hydrodynamic effects are known to lengthen the vibration period of the dam-reservoir system, and that this effect becomes more important as reservoir height and dam stiffness increase. The classical formulation and the proposed method are used to determine the influence of reservoir height on the variation of the period ratio $R_r = \tilde{T}_r/T_1$ where $\tilde{T}_r = 2\pi/\tilde{\omega}_r$ is the natural period of the dam-reservoir system, and $T_1 = 2\pi/\omega_1$ is the natural period of dam with an empty reservoir. The results obtained for two modulus of elasticity $E_s = 25$ GPa and $E_s = 35$ GPa, different reflection coefficients α and reservoir heights $H_r \geq 0.5H_s$ are presented in Fig. 11. The proposed method provides accurate predictions of the resonant vibration frequency of the dam-reservoir system for different reservoir heights.

Estimating the damping ratio $\tilde{\xi}_r$ of the dam-reservoir ESDOF is also of interest. Fenves and Chopra (1984) developed an analytical expression to include the effects of an added damping due to dam-reservoir interaction and reservoir bottom wave absorption. The damping ratio $\tilde{\xi}_r$ of the ESDOF dam-reservoir system can then be found based on the damping ratio ξ_1 of the dam with an empty reservoir as follows

$$\tilde{\xi}_r = \frac{\tilde{\omega}_r}{\omega_1} \xi_1 - \frac{1}{2M_1} \left(\frac{\tilde{\omega}_r}{\omega_1} \right)^2 \text{Im} [B_1(\tilde{\omega}_r)] \quad (79)$$

Fig. 12 presents the variation of the damping ratio $\tilde{\xi}_r$ of the ESDOF dam-reservoir system as a function of reservoir height $H_r \geq 0.5H_s$. As before, different values of reflection coefficient α and two modulus of elasticity of dam concrete are considered. The curves obtained using the classical and the proposed method coincide for reservoirs with a high reflective bottom. As previously emphasized, very small differences between the two sets of results are observed as reservoir bottom wave absorption increases.

The analytical expressions presented in this section can be adapted to conduct a simplified earthquake analysis of gravity dams for purposes of preliminary design, a method initially proposed by Fenves and Chopra (1985). As discussed previously, the fundamental vibration period $\tilde{T}_r = 2\pi/\tilde{\omega}_r$ of the dam-reservoir system is identified by the first resonant peak of the fundamental mode response functions given by Eq. (59). The generalized coordinate corresponding to resonant frequency $\tilde{\omega}_r$ is given by

Eq. (68)

$$\bar{Z}_1^{(x)}(\tilde{\omega}_r) = \frac{-\tilde{L}_1}{-\tilde{\omega}_r^2 \tilde{M}_1 + i \tilde{\omega}_r \tilde{C}_1 + K_1} \quad (80)$$

where the generalized mass \tilde{M}_1 , generalized damping \tilde{C}_1 , and participation factor \tilde{L}_1 of the dam-reservoir ESDOF are defined by

$$\tilde{M}_1 = M_1 + \text{Re}[B_1(\tilde{\omega}_r)]; \quad \tilde{C}_1 = C_1 - \tilde{\omega}_r \text{Im}[B_1(\tilde{\omega}_r)]; \quad \tilde{L}_1 = L_1 + B_0(\tilde{\omega}_r) \quad (81)$$

Maximum response of the dam-reservoir ESDOF system to a horizontal earthquake ground motion can be approximated at each time instant by its static response under the effect of equivalent lateral forces f_1 applied at the upstream dam face (Clough and Penzien 1975; Fenves and Chopra 1987)

$$f_1(y) = \frac{\tilde{L}_1}{\tilde{M}_1} S_a(\tilde{T}_r, \tilde{\xi}_r) [\tilde{\mu}_s(y) \psi_1^{(x)}(y)] \quad (82)$$

where $S_a(\tilde{T}_r, \tilde{\xi}_r)$ is the pseudo-acceleration ordinate of the earthquake design spectrum at vibration period \tilde{T}_r and for damping ratio $\tilde{\xi}_r$ of the dam-reservoir ESDOF system, and where $\tilde{\mu}_s(y)$ approximates the mass of the dam per unit height including hydrodynamic effects. This added-mass can be expressed here as

$$\begin{aligned} \tilde{\mu}_s(y) &= \mu_s(y) - \frac{\text{Re}[\bar{p}_1(0, y, \tilde{\omega}_r)]}{\psi_1^{(x)}(y)} \\ &= \mu_s(y) - \frac{1}{\psi_1^{(x)}(y)} \sum_{n=1}^{N_r} \text{Re} \left\{ \bar{p}_{0n}^{(x)}(0, y, \tilde{\omega}_r) \left[F_{1n}(\omega) + \frac{G_{1n}(\omega)}{I_{0n}(\omega)} \right] \right\} \end{aligned} \quad (83)$$

in which Eq. (39) was used to determine the frequency response function of the hydrodynamic pressure due to fundamental vibration mode. Frequency response function $\bar{p}_{0n}^{(x)}(0, y, \tilde{\omega}_r)$ can be evaluated using Eq. (43) or (58). It is important to note that the minus sign in Eq. (83) corresponds to the orientation of the system of axes shown in Fig. 2. We also assume that the fundamental mode shape $\psi_1^{(x)}$ is positive as indicated on the same Figure. Denoting $F_{st} = \rho_r g H_r^2 / 2$ the total hydrostatic force exerted on dam face, we determine the normalized equivalent lateral forces $H_s f_1(y) / [F_{st} S_a(\tilde{T}_r, \tilde{\xi}_r)]$ considering different reservoir bottom wave absorption levels and two modulus of elasticity of the one-meter wide dam section described previously. Fig. 13 shows that the results obtained using the classical formulation and the proposed method are identical. We note that the value of the equivalent lateral force is null at the dam crest because of the triangular shape of the dam monolith, this would not be the case in general. Finally, Fenves and Chopra (1985) discussed the effects of higher vibration modes on dam earthquake response. Using a static correction technique, this effect can be accounted for approximately by evaluating the static response of the dam-reservoir ESDOF subjected to the lateral forces f_{sc}

$$f_{sc}(y) = \ddot{x}_g^{(\max)} \left\{ \mu_s(y) \left[1 - \frac{L_1}{M_1} \psi_1^{(x)}(y) \right] - \left[\hat{p}_0^{(x)}(y) + \frac{\hat{B}_1}{M_1} \mu_s(y) \psi_1^{(x)}(y) \right] \right\} \quad (84)$$

where $\ddot{x}_g^{(\max)}$ denotes the maximum ground acceleration, and $\hat{p}_0^{(x)}(y)$ the real-valued, frequency independent hydrodynamic pressure applied on a rigid dam subjected to unit ground acceleration, with water compressibility neglected

$$\hat{p}_0^{(x)}(y) = -8\rho_r H_r \sum_{n=1}^{N_r} \frac{(-1)^{n-1}}{(2n-1)^2 \pi^2} \cos \left[\frac{(2n-1)\pi y}{2H_r} \right] \quad (85)$$

and where the term \hat{B}_1 is given by

$$\begin{aligned} \hat{B}_1 &= - \int_0^{H_r} \hat{p}_0^{(x)}(y) \psi_1^{(x)}(y) dy \\ &\approx 0.2 \frac{F_{st}}{g} \left(\frac{H_r}{H_s} \right)^2 \end{aligned} \quad (86)$$

The total earthquake response of the dam can then be determined by applying the SRSS rule to combine response quantities associated with the fundamental and higher vibration modes.

5 Conclusions

This paper presented and validated a practical and efficient formulation to evaluate the dynamic response of gravity dams impounding semi-infinite reservoirs with rectangular shapes. The proposed method uses closed-form analytical expressions to relate hydrodynamic pressure due to any deflected modal response of a 2D gravity dam on a rigid foundation to hydrodynamic pressure caused by a horizontal rigid body motion. Effects of dam flexibility, water compressibility and wave absorption at reservoir bottom are included in the formulation. New analytical expressions that can be easily programmed in a spreadsheet package or implemented in a dam structural analysis program were also proposed to conduct simplified fundamental mode earthquake analysis of gravity dams. The assumptions adopted to develop the formulas were first validated, and then numerical examples illustrating their use were presented. The proposed formulas were shown efficient to determine the frequency response functions of hydrodynamic pressure and dam acceleration, the heightwise distributions of hydrodynamic pressure, the dynamic properties of an equivalent dam-reservoir system and the associated equivalent lateral forces. The results obtained were compared to classical solutions based on iterative numerical schemes. The agreement between the two sets of results is excellent namely for reservoirs with common high to moderate levels of reservoir bottom wave reflection. The techniques presented in this paper can be efficiently used to provide valuable insights into the effects and relative importance of the various parameters involved in the dynamic response of dam-reservoir systems. Although the mathematical derivations and closed-form expressions developed were applied to dam-reservoir systems herein, they can be easily adapted to other fluid-structure interaction problems.

Acknowledgements

The authors would like to acknowledge the financial support of the Natural Sciences and Engineering Research Council of Canada (NSERC) and the Quebec Fund for Research on Nature and Technology (FQRNT).

Appendix A

Order of the approximation F_{jn} and G_{jn} expressions

Quadratic approximation

$$\psi_j^{(x)}(y) = \sum_{k=1}^2 a_k \left(\frac{y}{H_s} \right)^k$$

$$F_{jn}(\omega) = \psi_j^{(x)}(H_r) - \frac{2}{\lambda_n^2 H_s^2} a_2$$

$$G_{jn}(\omega) = -\frac{i\omega q}{\lambda_n^2 H_r} \left[\psi_j^{(x)}(H_r) \right] - \frac{1}{\lambda_n^2 H_r H_s} a_1$$

Cubic approximation

$$\psi_j^{(x)}(y) = \sum_{k=1}^3 a_k \left(\frac{y}{H_s} \right)^k$$

$$F_{jn}(\omega) = \psi_j^{(x)}(H_r) - \frac{2}{\lambda_n^2 H_s^2} a_2 - \frac{6H_r}{\lambda_n^2 H_s^3} a_3$$

$$G_{jn}(\omega) = -\frac{i\omega q}{\lambda_n^2 H_r} \left[\psi_j^{(x)}(H_r) - \frac{6H_r}{\lambda_n^2 H_s^3} a_3 \right] - \frac{1}{\lambda_n^2 H_r H_s} a_1 + \frac{6}{\lambda_n^4 H_r H_s^3} a_3$$

Quartic approximation

$$\psi_j^{(x)}(y) = \sum_{k=1}^4 a_k \left(\frac{y}{H_s} \right)^k$$

$$F_{jn}(\omega) = \psi_j^{(x)}(H_r) - \frac{2}{\lambda_n^2 H_s^2} a_2 - \frac{6H_r}{\lambda_n^2 H_s^3} a_3 + \left(\frac{24}{\lambda_n^4 H_s^4} - \frac{12H_r^2}{\lambda_n^2 H_s^4} \right) a_4$$

$$G_{jn}(\omega) = -\frac{i\omega q}{\lambda_n^2 H_r} \left[\psi_j^{(x)}(H_r) - \frac{6H_r}{\lambda_n^2 H_s^3} a_3 - \frac{12H_r^2}{\lambda_n^2 H_s^4} a_4 \right]$$

$$- \frac{1}{\lambda_n^2 H_r H_s} a_1 + \frac{6}{\lambda_n^4 H_r H_s^3} a_3$$

Quintic approximation

$$\psi_j^{(x)}(y) = \sum_{k=1}^5 a_k \left(\frac{y}{H_s} \right)^k$$

$$F_{jn}(\omega) = \psi_j^{(x)}(H_r) - \frac{2}{\lambda_n^2 H_s^2} a_2 - \frac{6H_r}{\lambda_n^2 H_s^3} a_3 + \left(\frac{24}{\lambda_n^4 H_s^4} - \frac{12H_r^2}{\lambda_n^2 H_s^4} \right) a_4$$

$$+ \left(\frac{120H_r}{\lambda_n^4 H_s^5} - \frac{20H_r^3}{\lambda_n^2 H_s^5} \right) a_5$$

$$G_{jn}(\omega) = -\frac{i\omega q}{\lambda_n^2 H_r} \left[\psi_j^{(x)}(H_r) - \frac{6H_r}{\lambda_n^2 H_s^3} a_3 - \frac{12H_r^2}{\lambda_n^2 H_s^4} a_4 + \left(\frac{120H_r}{\lambda_n^4 H_s^5} - \frac{20H_r^3}{\lambda_n^2 H_s^5} \right) a_5 \right]$$

$$- \frac{1}{\lambda_n^2 H_r H_s} a_1 + \frac{6}{\lambda_n^4 H_r H_s^3} a_3 - \frac{120}{\lambda_n^6 H_r H_s^5} a_5$$

References

- ADINA Research and Development, Inc. (2003). "Theory and modeling guide, Volume I: ADINA Solids and Structures." *Report ARD 08-7*, Watertown, Massachusetts.
- Bouaanani, N., Paultre, P., and Proulx, J. (2002). "Two-dimensional modelling of ice-cover effects for the dynamic analysis of concrete gravity dams." *Earthquake Engineering and Structural Dynamics*, 31(12), 2083–2102.
- Bouaanani, N., Paultre, P., and Proulx, J. (2003). "A closed-form formulation for earthquake-induced hydrodynamic pressure on gravity dams." *Journal of Sound and Vibration*, 261(3), 573–582.
- Chakrabarti, P., and Chopra, A. K. (1973). "Earthquake analysis of gravity dams including hydrodynamic interaction." *Earthquake Engineering and Structural Dynamics*, 2(2), 143–160.
- Chopra, A. K. (1968). "Earthquake behavior of reservoir-dam systems." *Journal of the Engineering Mechanics Division, ASCE*, 94(6), 1475–1500.
- Chopra, A. K. (1970). "Earthquake response of concrete gravity dams." *Report No. UCB/EERC-70/01*, University of California, Berkeley, California.
- Chopra, A. K. (1978). "Earthquake resistant design of concrete gravity dams." *Journal of the Structural Division, ASCE*, 104(6), 953–971.
- Clough, R. W., and Penzien, J. (1975). "Dynamics of structures." Mc-Graw-Hill, Inc., New York.
- Fennes, G., and Chopra, A. K. (1984). "EAGD-84, a computer program for earthquake analysis of concrete gravity dams." *Report No. UCB/EERC-84/11*, University of California, Berkeley, California.
- Fennes, G., and Chopra, A. K. (1985). "Simplified earthquake analysis of concrete gravity dams: Separate hydrodynamic and foundation interaction effects." *Journal of Engineering Mechanics, ASCE*, 111(6), 715–735.
- Fennes, G., and Chopra, A. K. (1987). "Simplified earthquake analysis of concrete gravity dams." *Journal of Structural Engineering, ASCE*, 113(8), 1688–1708.
- Fok, K. L., Hall, J. F., and Chopra, A. K. (1986). "EACD-3D, a computer program for three-dimensional earthquake analysis of concrete dams." *Report No. UCB/EERC-86/09*, University of California, Berkeley, California.
- Hall, J. F. and Chopra, A. K. (1980). "Dynamic response of embankment, concrete-gravity and arch dams including hydrodynamic interaction." *Report No. UCB/EERC-80/39*, University of California, Berkeley, California.
- Humar, J. L. and Jablonski, A. M. (1988). "Boundary element reservoir model for seismic analysis of gravity dams." *Earthquake Engineering and Structural Dynamics*, 16(8), 1129–1156.

- Liu, Ph., and Cheng, A. (1984). "Boundary solutions for fluid-structure interaction." *Journal of Hydraulic Engineering, ASCE*, 110(01), 51–64.
- Maeso, O., Aznarez, J. J., and Dominguez, J. (2004). "Three-dimensional models of reservoir sediment and effects on the seismic response of arch dams." *Earthquake Engineering and Structural Dynamics*, 33(10), 1103–1123.
- Proulx, J., Paultre, P., Rheault, J., and Robert, Y. (2000). "An experimental investigation of water level effects on the dynamic behaviour of a large arch dam." *Earthquake Engineering and Structural Dynamics*, 30(8), 1147–1166.
- Saini, S. S., Bettess, P., and Zienkiewicz, O. C. (1978). "Coupled hydrodynamic response of concrete gravity dams using finite and infinite elements." *Earthquake Engineering and Structural Dynamics*, 6(4), 363–374.
- Tsai, C. S., and Lee, G. C. (1987). "Arch dam-fluid interactions: by FEM-BEM and substructure concept." *International Journal of Numerical Methods in Engineering*, 24(12), 2367–2388.
- Westergaard, H. M. (1933). "Water pressure on dams during earthquakes." *Transactions, ASCE*, 98(1850), 418–472.

List of figures

- Fig. 1: Dam-reservoir system considered.
- Fig. 2: Approximation of dam mode shapes.
- Fig. 3: Absolute value of frequency response function of the flexible part of hydrodynamic pressure at dam heel corresponding to structural mode shapes 1 to 4, and to two values of wave reflection coefficient $\alpha = 0.95$ and $\alpha = 0.65$; — Classical method; —□— Proposed method.
- Fig. 4: Variation of the real and imaginary parts of eigenvalues λ_n , $n = 1, 2, 3$, as a function of frequency ratio ω/ω_0 and considering different values of wave reflection coefficient α ; — Classical method; —□— Proposed method.
- Fig. 5: Variation of the real and imaginary parts of coefficients β_n , $n = 1, 2, 3$, as a function of frequency ratio ω/ω_0 and considering different values of wave reflection coefficient α ; — Classical method; —□— Proposed method.
- Fig. 6: Variation of the real and imaginary parts of coefficients κ_n , $n = 1, 2, 3$, as a function of frequency ratio ω/ω_0 and considering different values of wave reflection coefficient α ; — Classical method; —□— Proposed method.
- Fig. 7: Absolute value of frequency response functions of the rigid and flexible parts of hydrodynamic pressure at dam heel for different values of wave reflection coefficient α ; — Classical method; —□— Proposed method.
- Fig. 8: Absolute value of frequency response functions of horizontal acceleration at dam crest for different values of wave reflection coefficient α and two dam modulus of elasticity E_s ; — Classical method; —□— Proposed method.
- Fig. 9: Absolute value of frequency response functions of total hydrodynamic pressure at dam heel for different values of wave reflection coefficient α and two dam modulus of elasticity E_s ; — Classical method; —□— Proposed method.
- Fig. 10: Absolute value of the total hydrodynamic pressure distributions over reservoir height for different values of wave reflection coefficient α and two dam modulus of elasticity E_s ; — Classical method; —□— Proposed method.
- Fig. 11: Effect of reservoir height on the variation of the period ratio \tilde{T}_r/T_1 for different values of wave reflection coefficient α and two dam modulus of elasticity E_s ; — Classical method; —□— Proposed method.
- Fig. 12: Effect of reservoir height on the variation of the damping ratio $\tilde{\xi}_r$ for different values of wave reflection coefficient α and two dam modulus of elasticity E_s ; — Classical method; —□— Proposed method.
- Fig. 13: Equivalent lateral earthquake forces corresponding to dam fundamental mode response for different values of wave reflection coefficient α and two dam modulus of elasticity E_s ; — Classical method; —□— Proposed method.

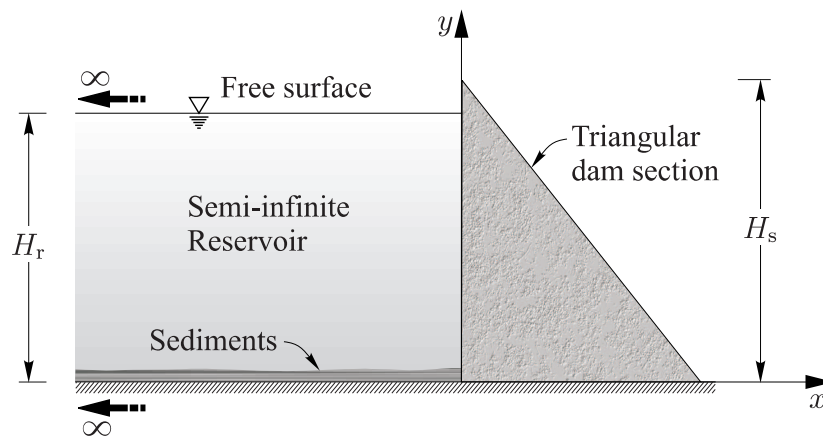


Figure 1. Dam-reservoir system considered.

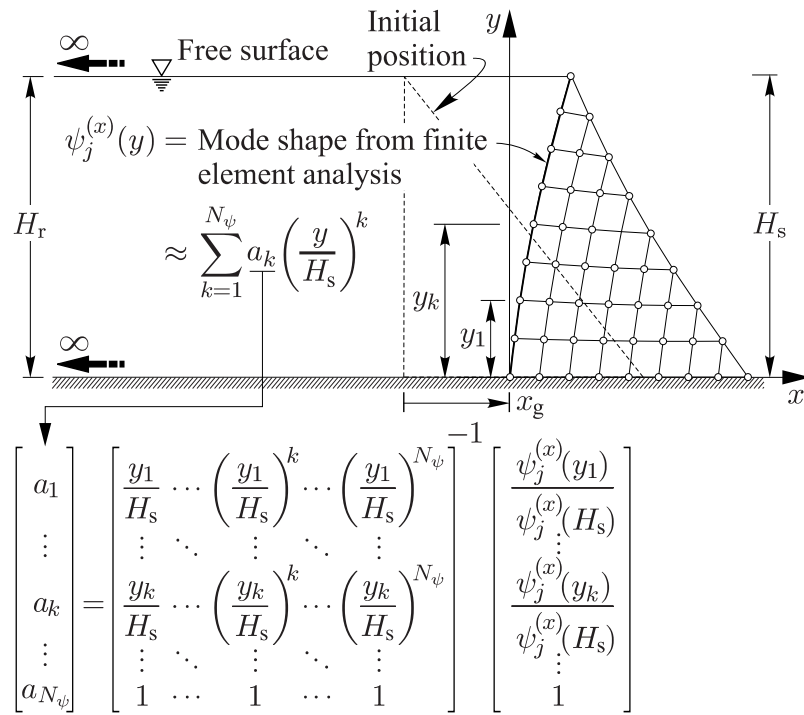


Figure 2. Approximation of dam mode shapes.

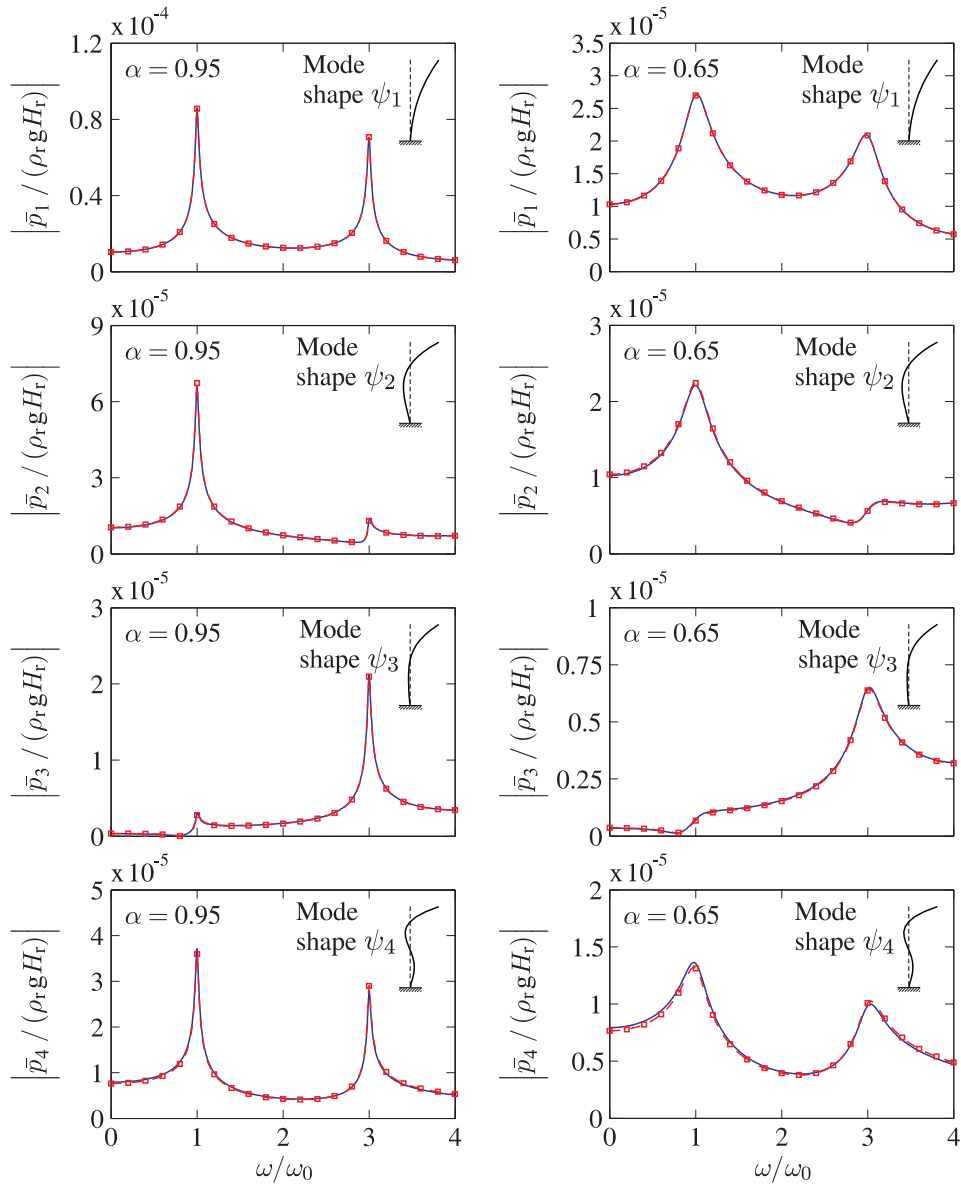


Figure 3. Absolute value of frequency response function of the flexible part of hydrodynamic pressure at dam heel corresponding to structural mode shapes 1 to 4, and to two values of wave reflection coefficient $\alpha = 0.95$ and $\alpha = 0.65$; — Classical method; —□— Proposed method.

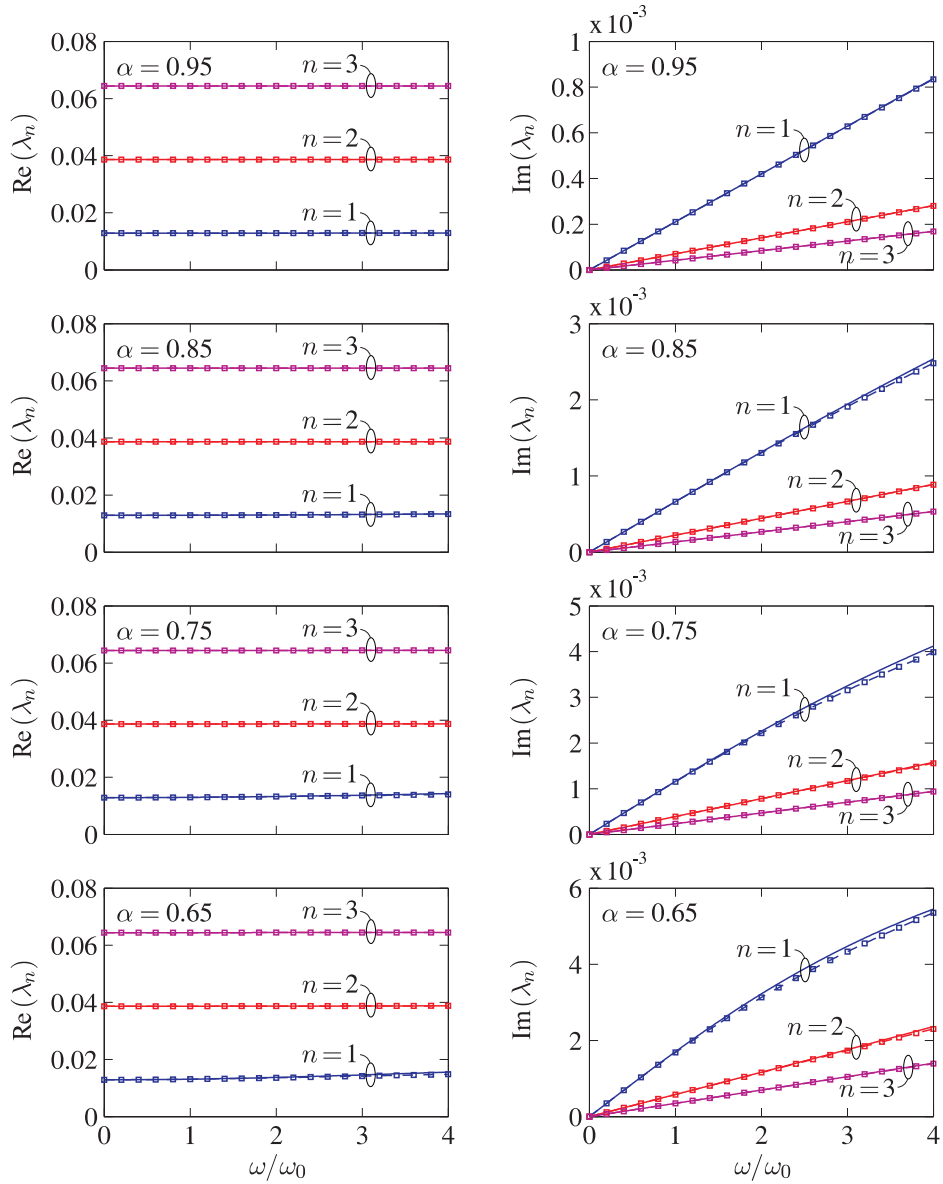


Figure 4. Variation of the real and imaginary parts of eigenvalues λ_n , $n = 1, 2, 3$, as a function of frequency ratio ω/ω_0 and considering different values of wave reflection coefficient α ; — Classical method; —□— Proposed method.

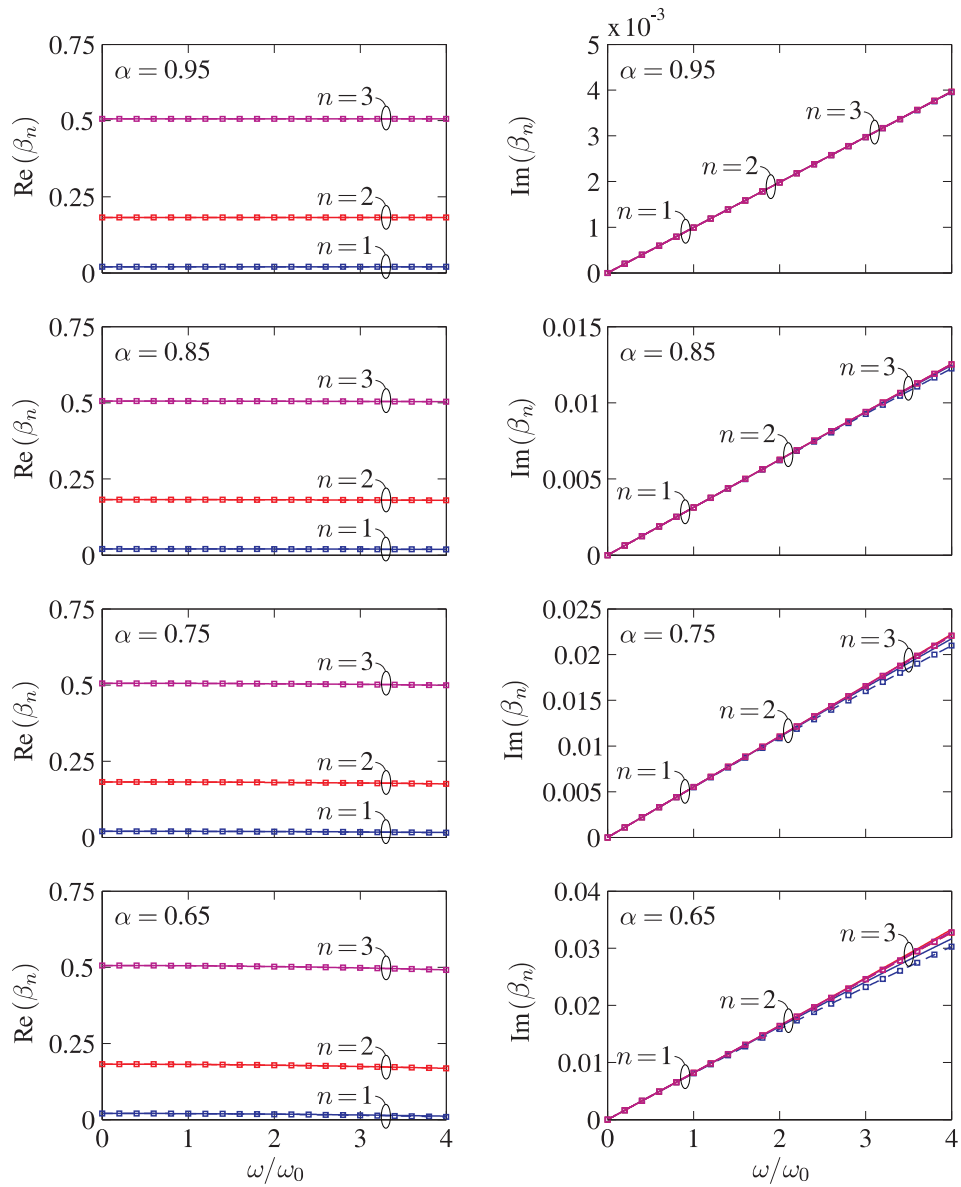


Figure 5. Variation of the real and imaginary parts of coefficients β_n , $n = 1, 2, 3$, as a function of frequency ratio ω/ω_0 and considering different values of wave reflection coefficient α ; — Classical method; —□— Proposed method.

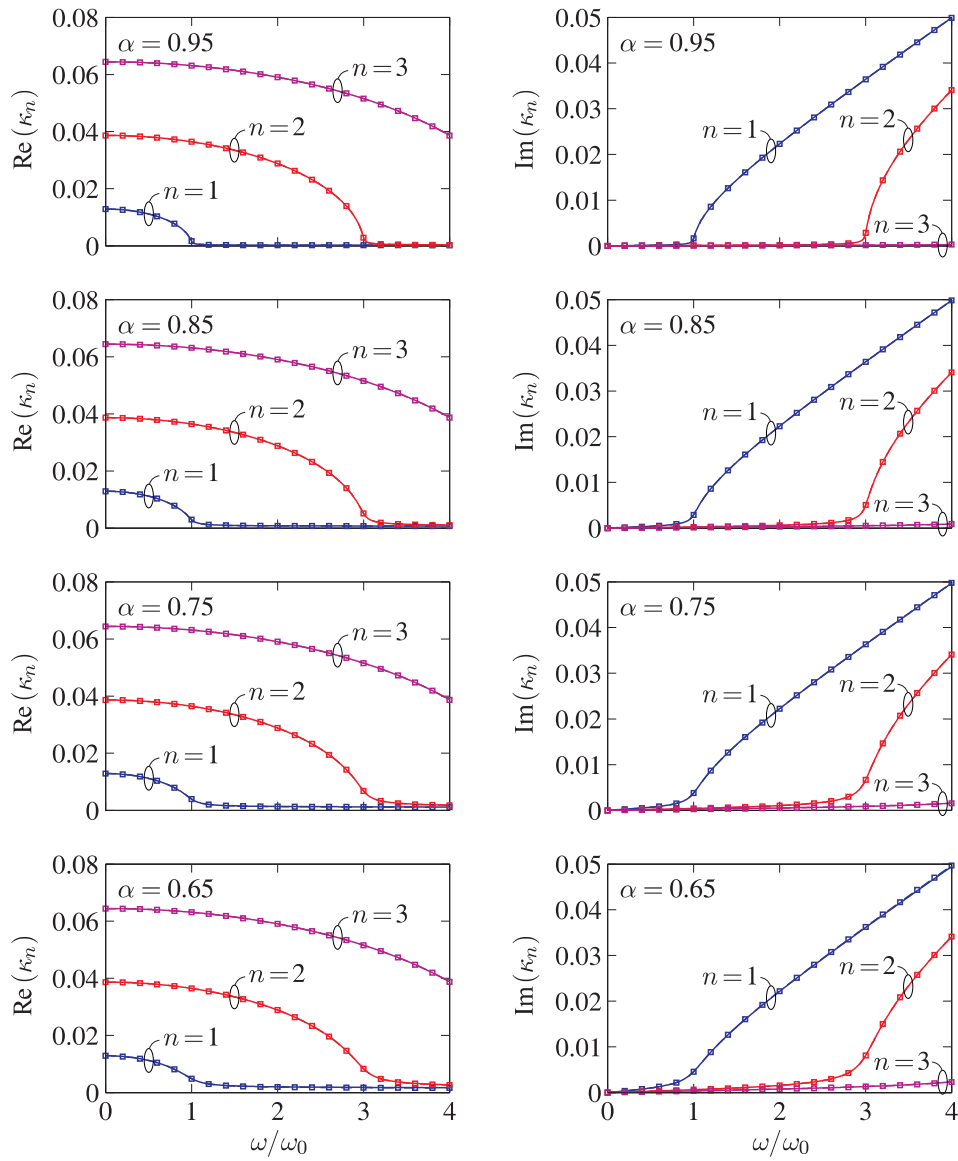


Figure 6. Variation of the real and imaginary parts of coefficients κ_n , $n = 1, 2, 3$, as a function of frequency ratio ω/ω_0 and considering different values of wave reflection coefficient α ; — Classical method; —□— Proposed method.

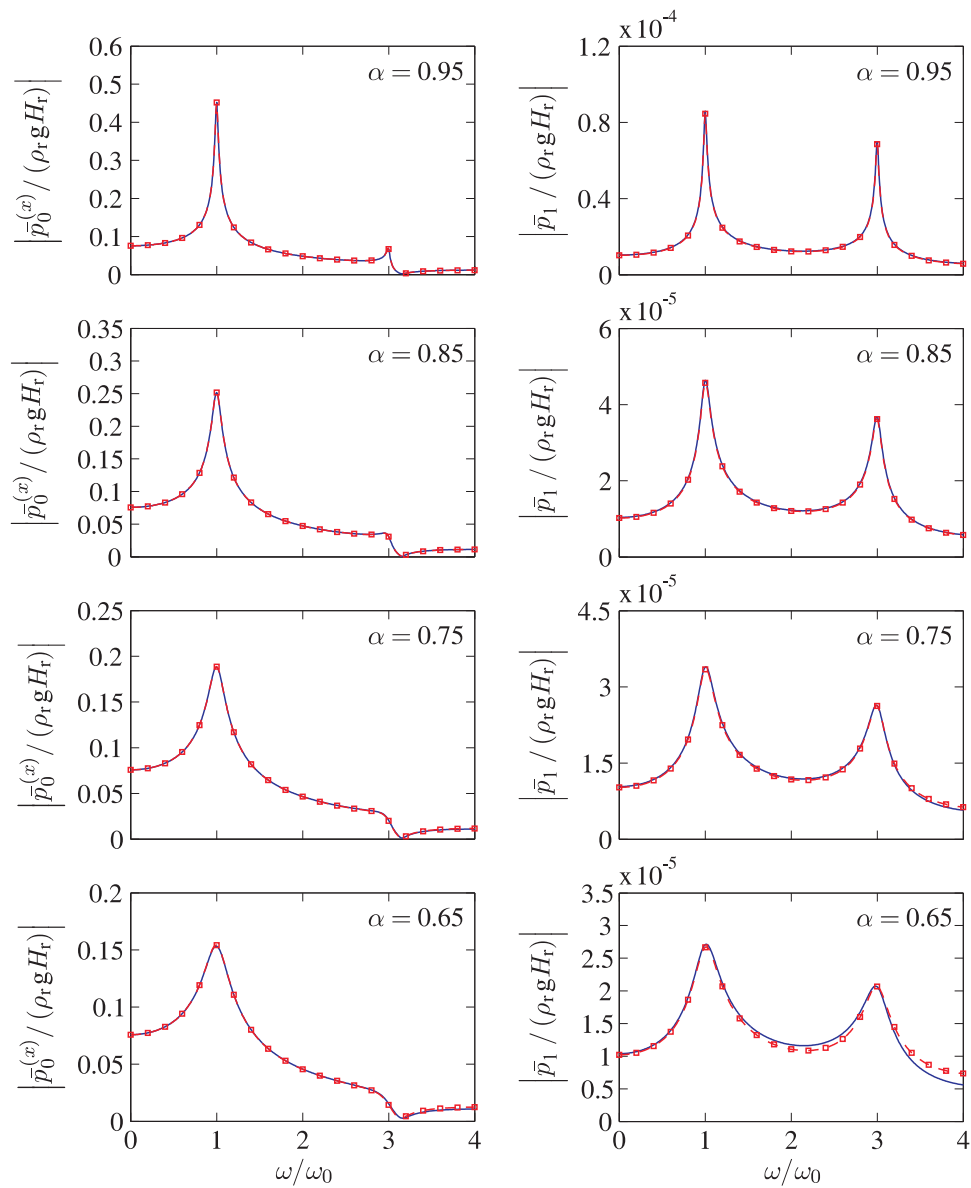


Figure 7. Absolute value of frequency response functions of the rigid and flexible parts of hydrodynamic pressure at dam heel for different values of wave reflection coefficient α ; — Classical method; —□— Proposed method.

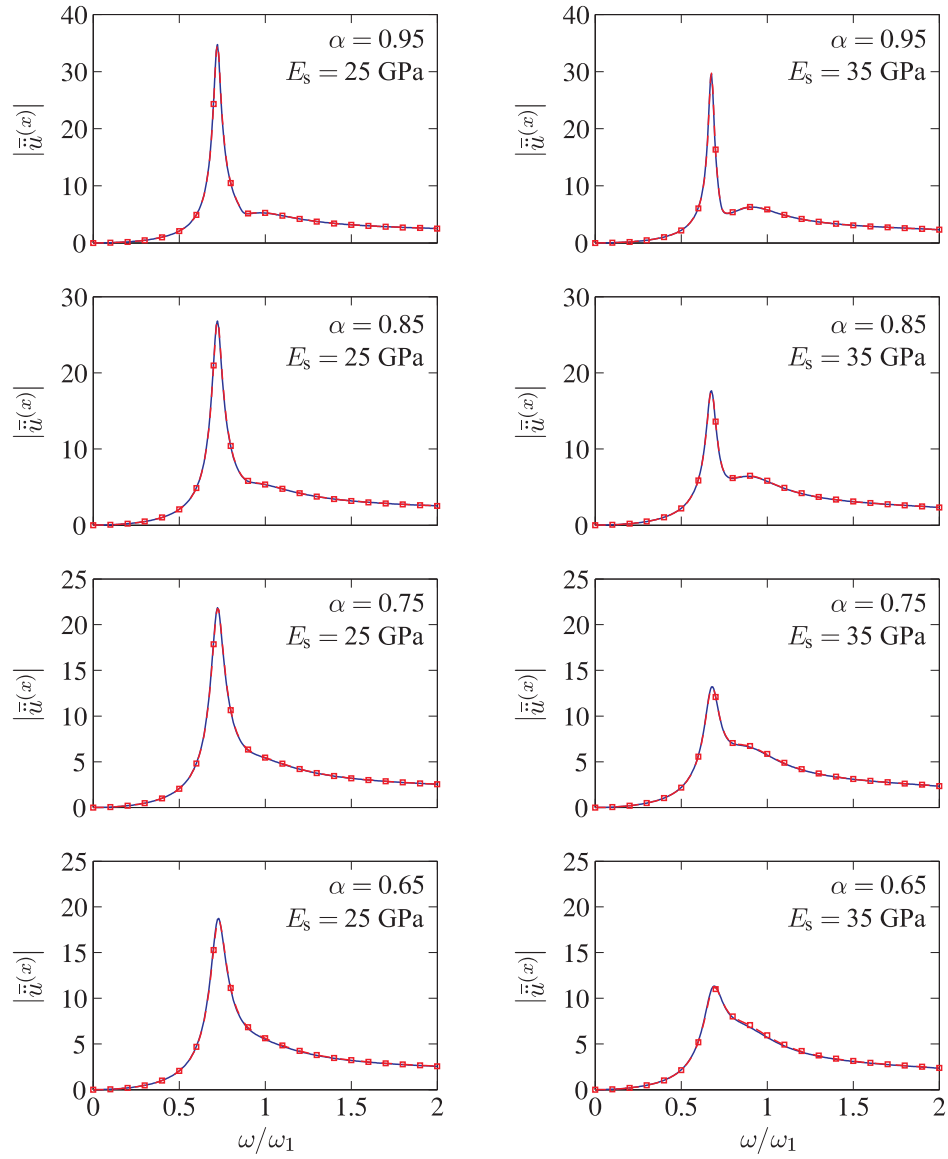


Figure 8. Absolute value of frequency response functions of horizontal acceleration at dam crest for different values of wave reflection coefficient α and two dam modulus of elasticity E_s ; — Classical method; —□— Proposed method.

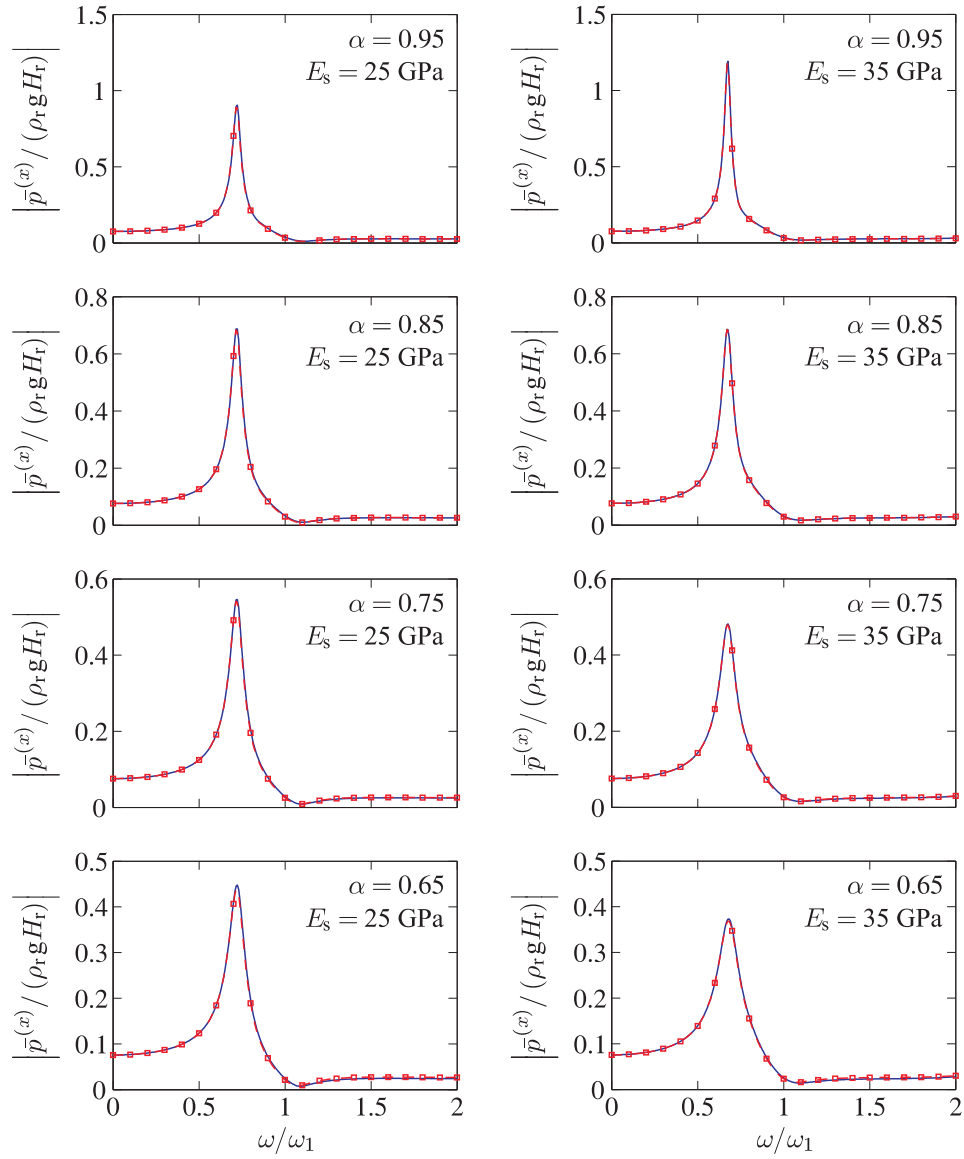


Figure 9. Absolute value of frequency response functions of total hydrodynamic pressure at dam heel for different values of wave reflection coefficient α and two dam modulus of elasticity E_s ; — Classical method; —□— Proposed method.

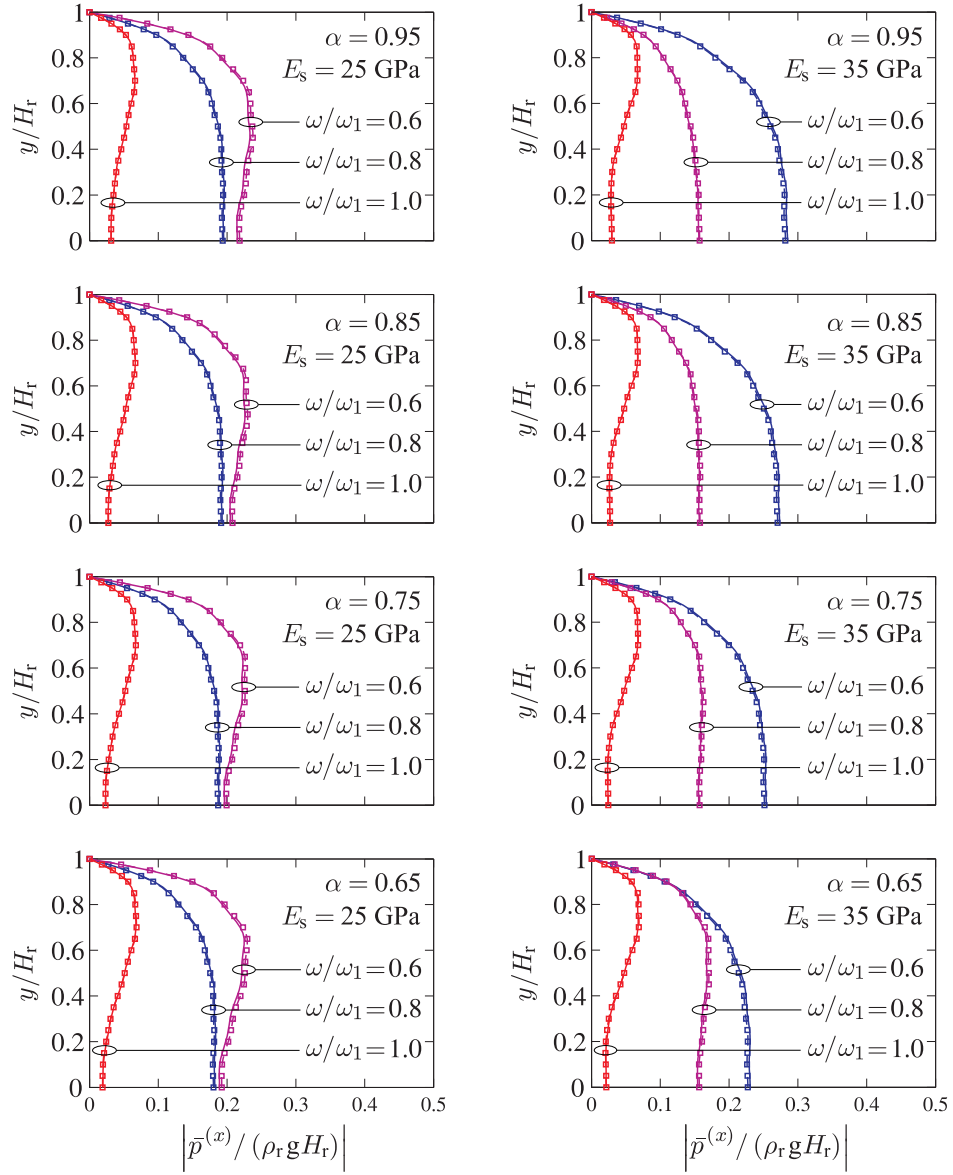


Figure 10. Absolute value of the total hydrodynamic pressure distributions over reservoir height for different values of wave reflection coefficient α and two dam modulus of elasticity E_s ; — Classical method; —□— Proposed method.

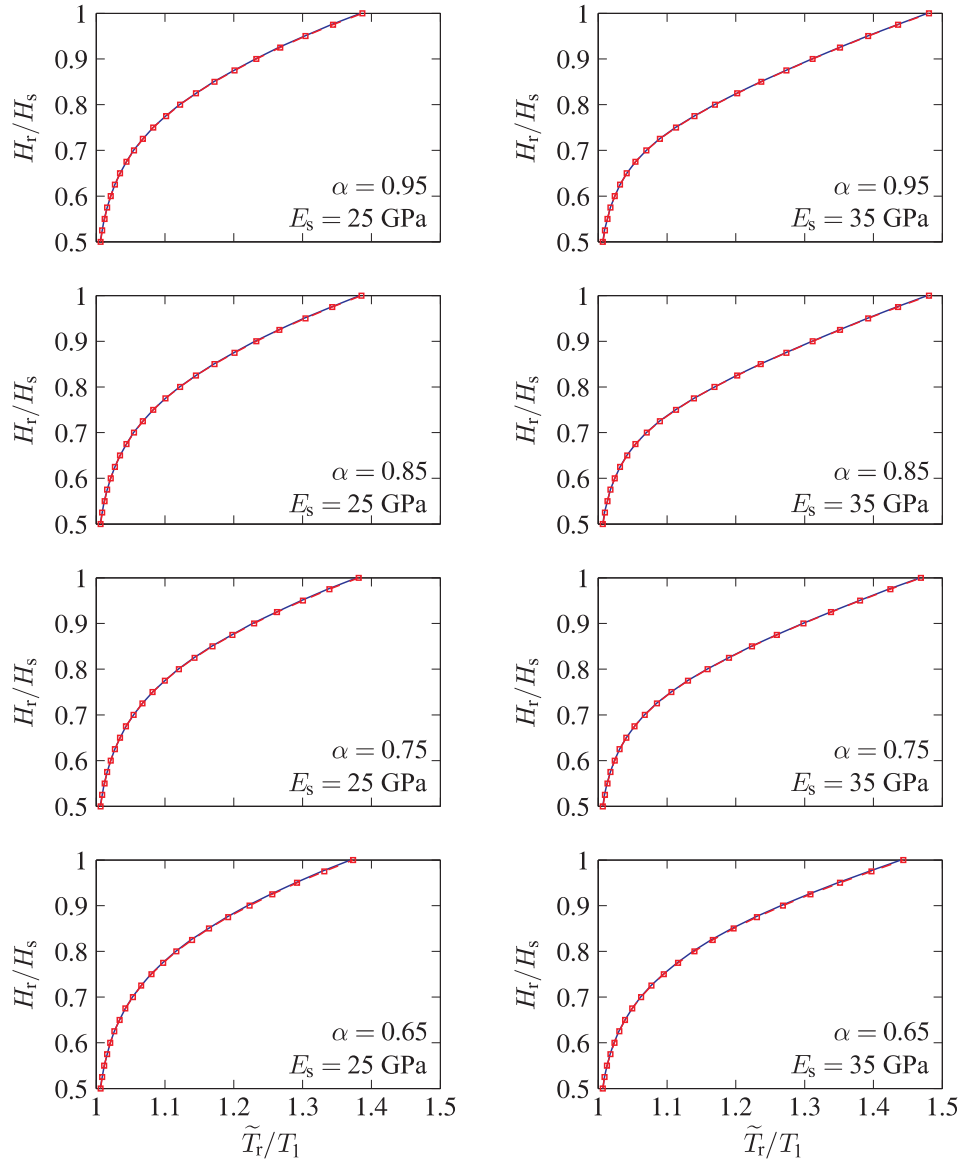


Figure 11. Effect of reservoir height on the variation of the period ratio \tilde{T}_r/T_1 for different values of wave reflection coefficient α and two dam modulus of elasticity E_s ; — Classical method; —□— Proposed method.

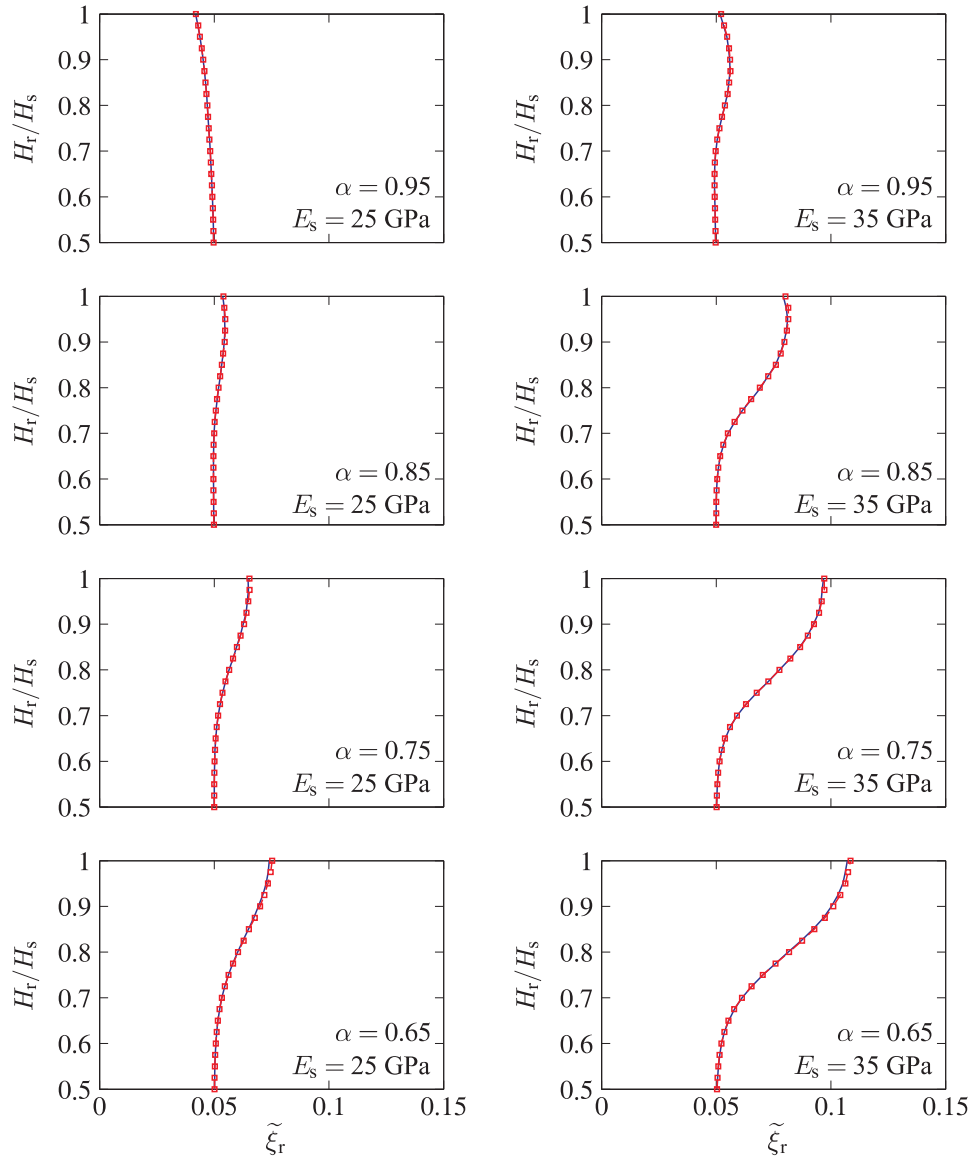


Figure 12. Effect of reservoir height on the variation of the damping ratio $\tilde{\xi}_r$ for different values of wave reflection coefficient α and two dam modulus of elasticity E_s ; — Classical method; —□— Proposed method.

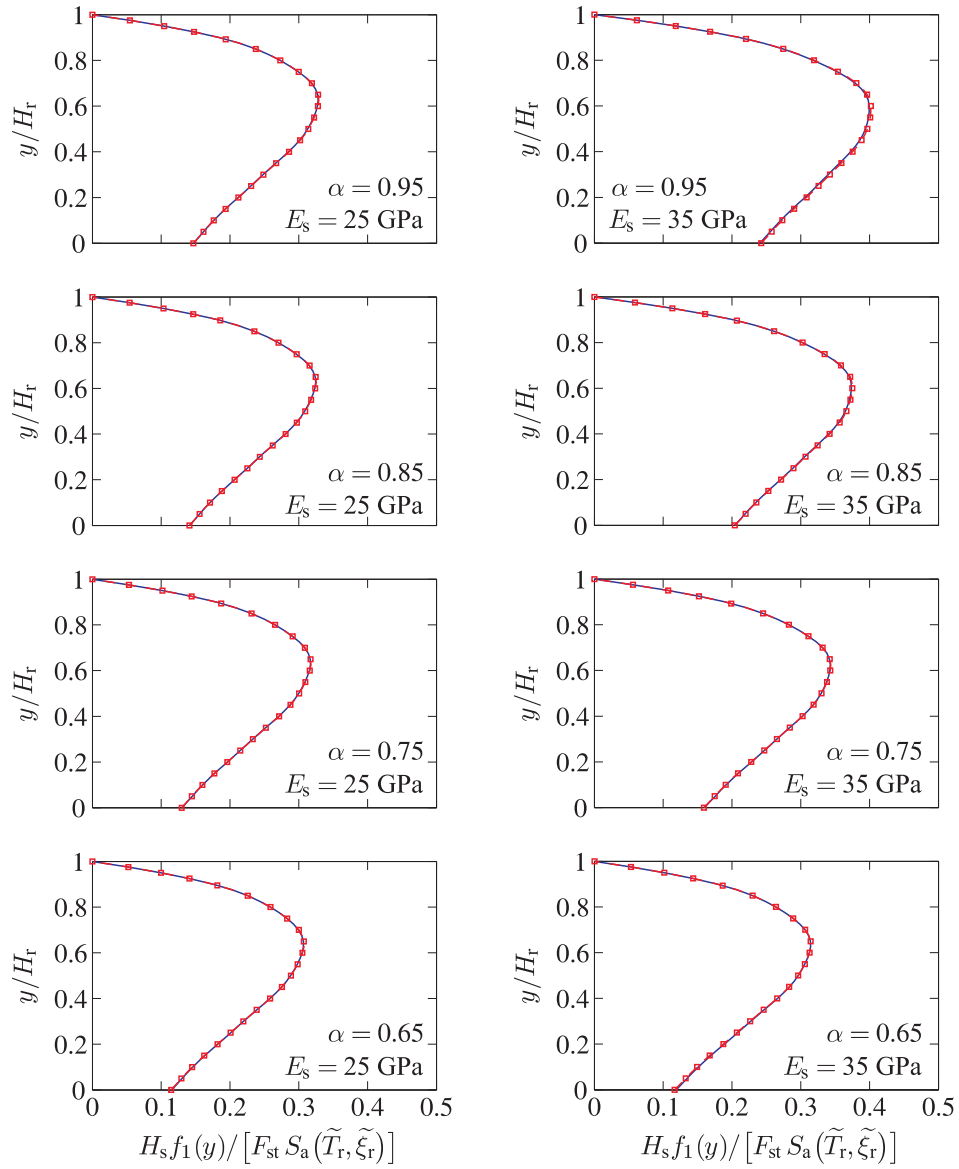


Figure 13. Equivalent lateral earthquake forces corresponding to dam fundamental mode response for different values of wave reflection coefficient α and two dam modulus of elasticity E_s ; — Classical method; —□— Proposed method.